From Graphene to Silicene: Topological Phase Diagram and Transition

Motohiko Ezawa
Department of Applied Physics
University of Tokyo

EQPCM Symposium

Outline

- Silicene is a graphene-like silicon structure
- It has a rich variety of topological phases induced by applying various external fields
- They are QSH, QAH, hybrid QSQAH insulators
- There appear topological (semi)metals such as single-Dirac cone state and valley-polarized metal

➢ DOS & quantized conductance of edge channels

➢ Experimental observations by STM/STS, ARPES

Silicene

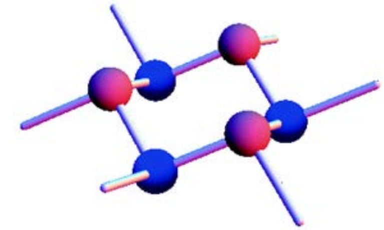

- Silicene is a monolayer of silicon atoms forming 2-dimensional honeycomb lattice

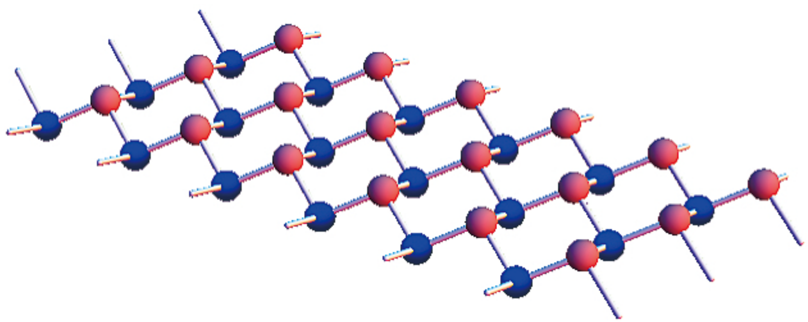

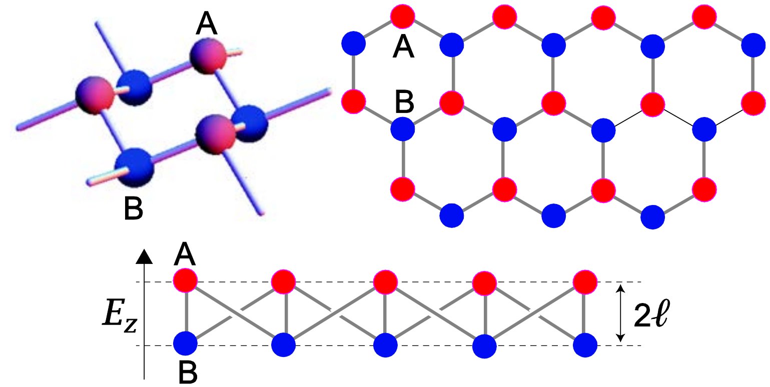

- K. Takeda and K. Shiraishi, Phys. Rev. B 50, 075131 (1994).
- G. G. Guzm´an-Verri and L. C. Lew Yan Voon, Phys. Rev. B **76**, 075131 (2007).
- C-C. Liu, W. Feng, and Y. Yao, PRL 107, 076802 (2011)
- C-C. Liu, H.Jiang and Y. Yao, PRB **84** 195430 (2011)

My Works on Silicene

15 papers including
2 PRL

1. "*Topological Insulator and Helical Zero Mode in Silicene under Inhomogeneous Electric Field* ,
M. Ezawa, New J. Phys. 14, 033003 (2012)
2. "*Quantum Hall Effects in Silicene*", M. Ezawa, J. Phys. Soc. Japan 81, 064705 (2012)
3. "*Quantum Anomalous Hall Effects and Valley-Polarized Metals in Silicene*" M. Ezawa, Phys. Rev. Lett 109, 055502 (2012)
4. "*Dirac Theory and Topological Phases of Silicon Nanotube*" M. Ezawa, Europhysics Letters 98, 67001 (2012)
5. "*Quasi-Topological Insulator and Trigonal Warping in Gated Bilayer Silicene*", M. Ezawa, J. Phys. Soc. Jpn. 81, 104713 (2012)
6. "*Topological Phase Transition and Electrically Tunable Diamagnetism in Silicene*" M. Ezawa, Euro. Phys. J. B 85, 363 (2012)
7. "*Spin-Valley Optical Selection Rule and Strong Circular Dichroism in Silicene*" M. Ezawa, Phys. Rev. B 86, 161407(R)
8. "*Photo-Induced Topological Phase Transition and Single Dirac-Cone State in Silicene*"
M. Ezawa, Phys. Rev. Lett 110, 026603 (2013)
9. "*Hexagonally Warped Dirac Cones and Topological Phase Transition in Silicene Superstructure*"
M. Ezawa, Euro. Phys. J. B 86, 139 (2013)
10. "*Spin-Valleytronics in Silicene: Quantum-Spin-Quantum-Anomalous Hall Insulators and Single-Valley Semimetals*"
M. Ezawa, Phys. Rev. B 87, 155415 (2013)
11. "*Interference of Topologically Protected Edge States in Silicene Nanoribbons*" M. Ezawa and N. Nagoasa, cond-mat/arXiv:1301.6337
12. "*Half-Integer Quantum Hall Effects in Silicene*" M. Ezawa, cond-mat/arXiv:1302.2284
13. "*Quantized Conductance and Field-Effect Topological Quantum Transistor in Silicene Nanoribbons*"
M. Ezawa, Appl. Phys. Lett. 102, 172103 (2013)
14. "*Charge Transport in a Silicene pn Junction*" A. Yamakage, M. Ezawa, Y. Tanaka and N. Nagaosa, cond-mat/arXiv:1303.1245
15. "Quantum Hall Effects with High Spin-Chern Numbers in Buckled Honeycomb Structure
with Magnetic Order" M. Ezawa, cond-mat/arXiv:1306.

Review on silicene

●内容の範囲
固体物理（結晶，アモルファス物質，金属物性，誘電体，半導体，磁性体，光学的・熱的・機械的性質 など） 固体物理の応用（半導体素子，磁性材料，光学的結晶材料，レーザー など） 実験法・実験装置（分析・計測機器，自動化機器，計算機 など） 固体物理周辺の最近の話題 そのほか（随想，内外ニュース，書籍の紹介 など）

固体物理

２０１３年４月・第48巻 第４号

トピックス

グラフェンからシリセンへ：シリコンでできたトポロジカル絶縁体

東京大学大学院工学系研究科　江澤雅彦

SOLID STATE PHYSICS

April 2013

Vol. 48, No. 4

published monthly by
AGNE GIJUTSU CENTER

Kitamura Bldg.
1–25, Minamiaoyama
5 chome,
Minato-ku, Tokyo

CONTENTS

ARPES of Silicene

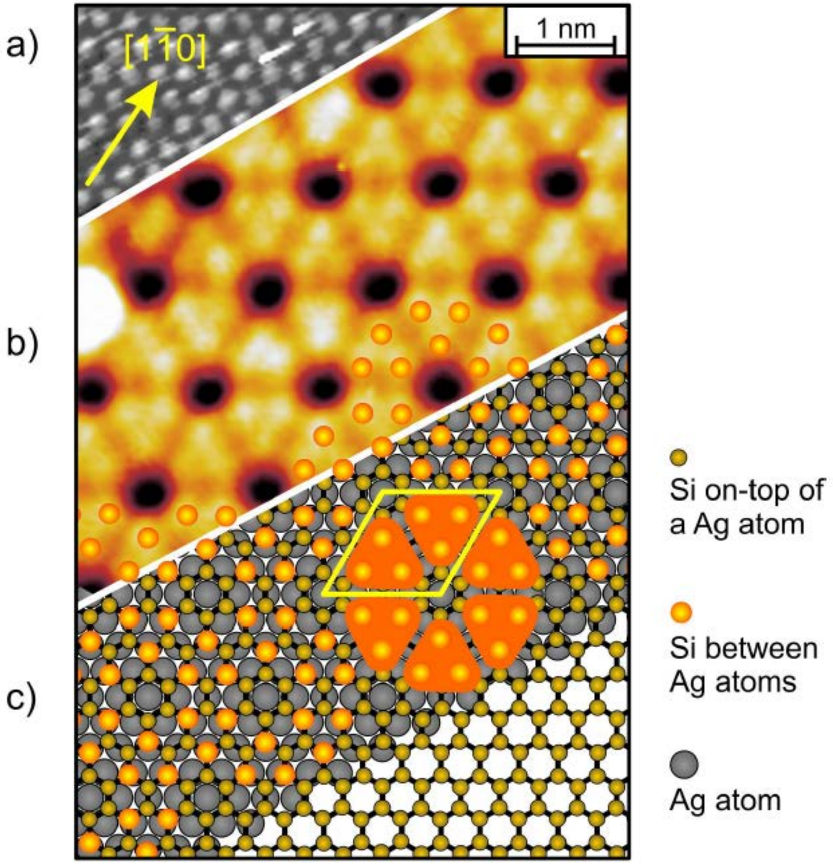

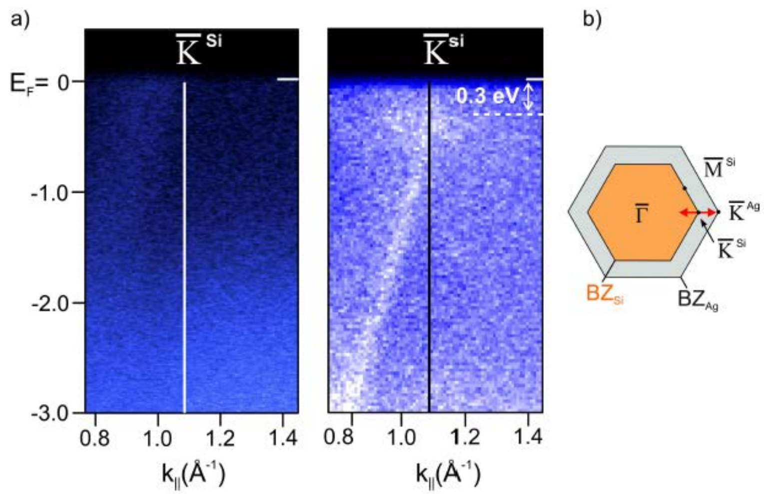

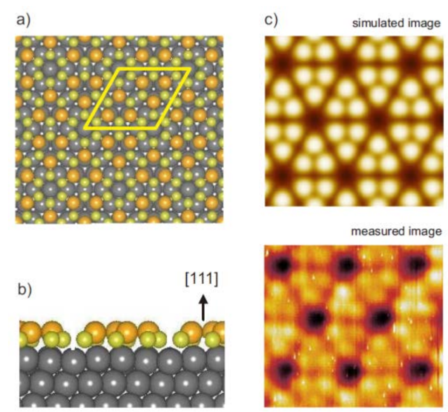

Guy Le Lay et al, Phys. Rev. Lett. 108, 155501 (2012)

Presence of gapped silicene-derived band in the prototypical (3x3) silicene phase on silver (111) surfaces

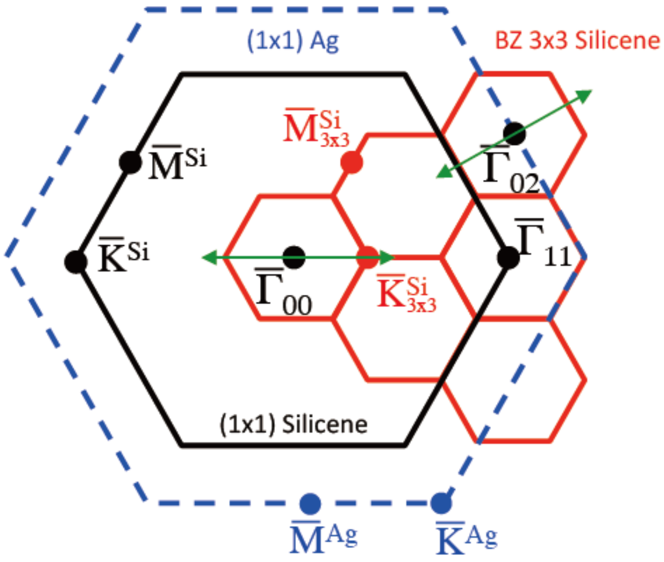

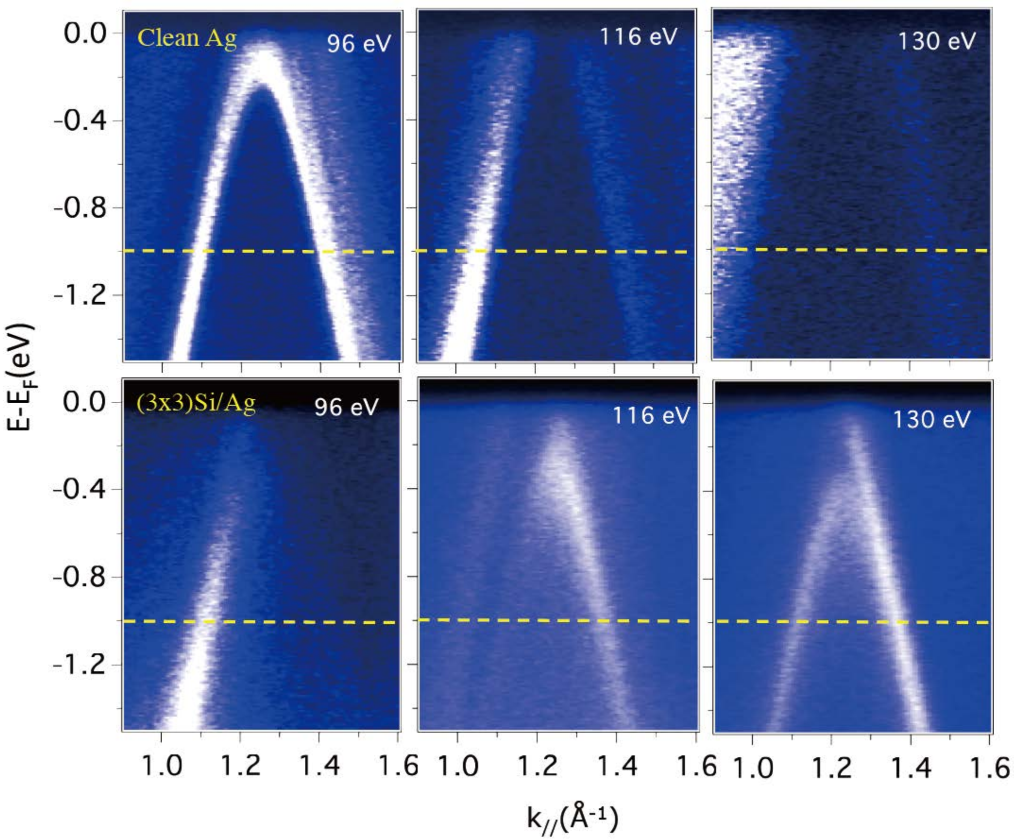

G. L. Lay, et. al. J. Phys. C (to be published)

STM and LEED Experiments

- Low-energy electron diffraction

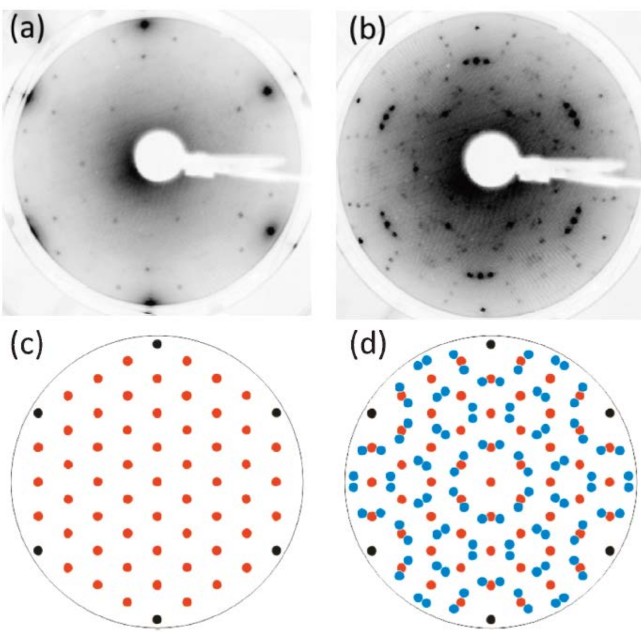

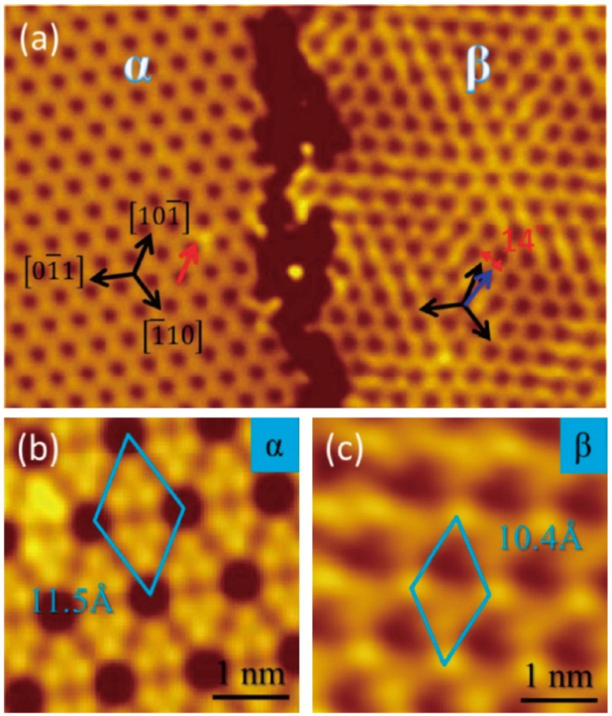

N. Takagi, M. Kawai et.al., Appl. Phys. Express 5, 045802 (2012) .

Silicene on ZrB2

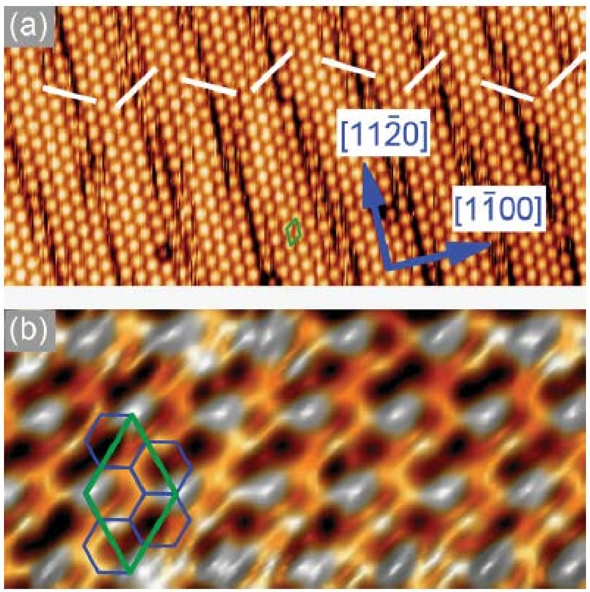

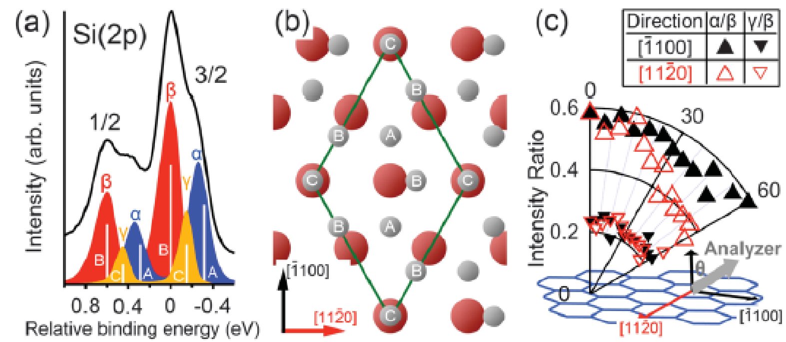

zirconium diboride

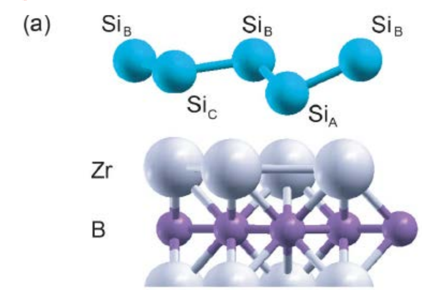

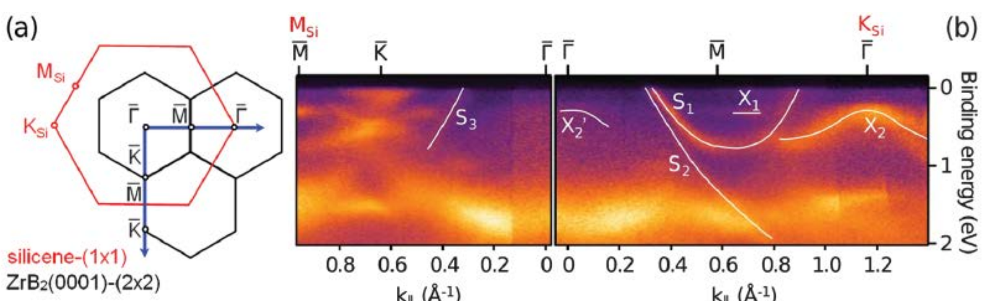

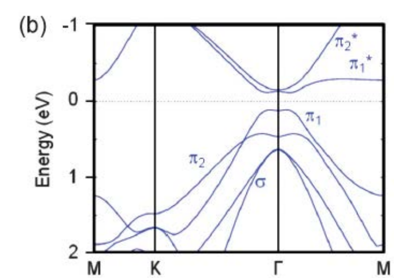

Y. Takamura, et.al. PRL 108, 245501 (2012)

Silicene on Ir(111)

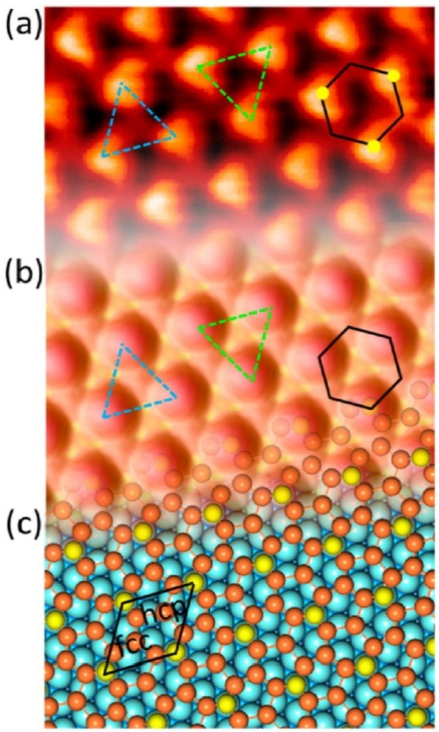

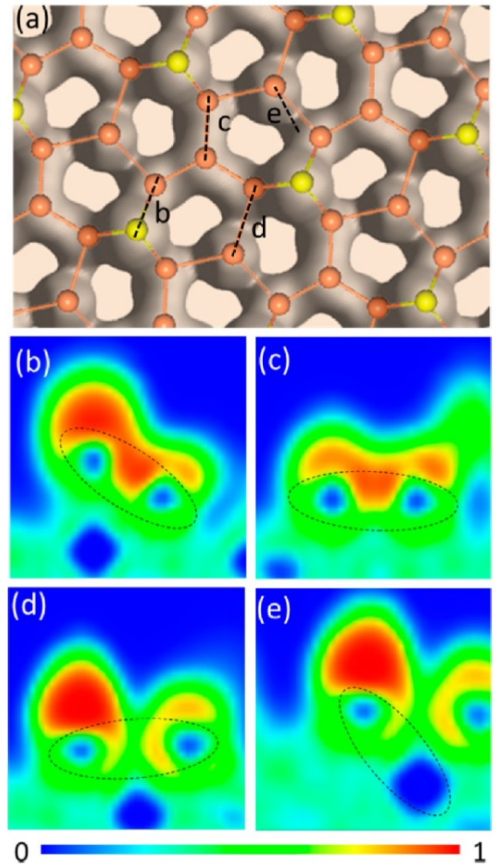

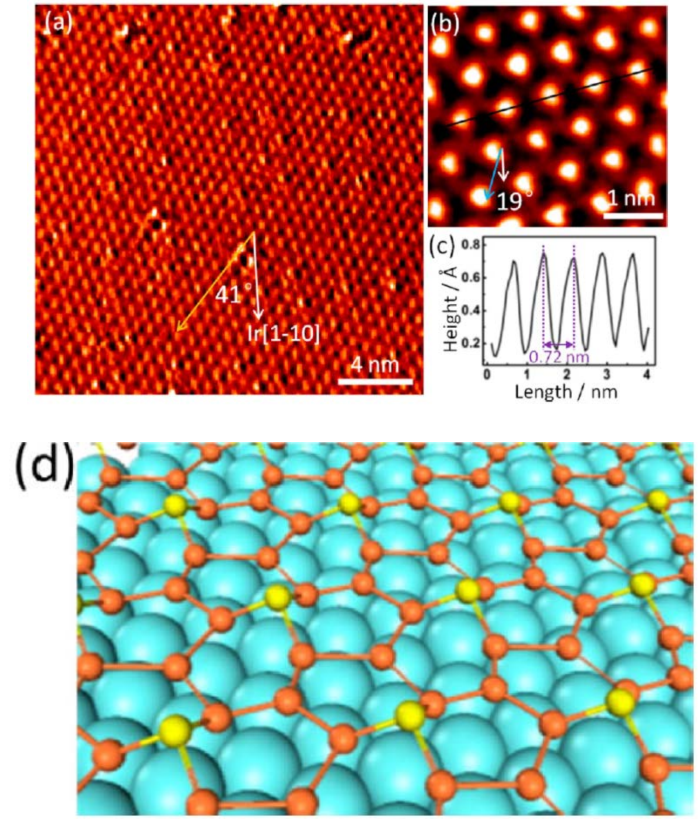

Meng et al NanoLett. 13, 685 (2013)

Experiment on Bilayer Silicene

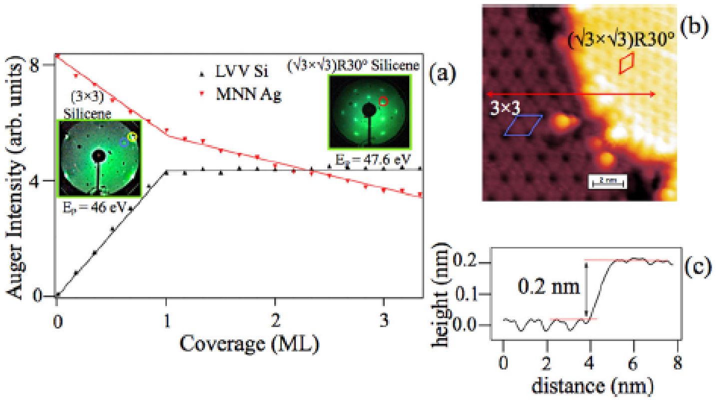

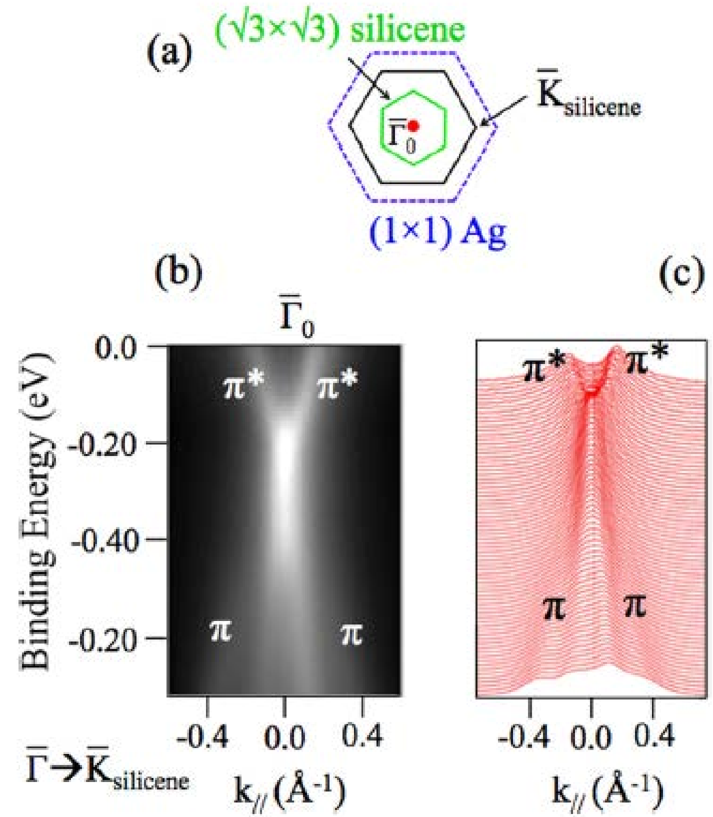

S. Hasegawa and G. L. Lay, et.al, Appl. Phys. Lett. 102, 163106 (2013)

Silicene and Germanene

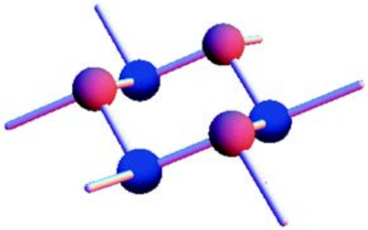

C Si Ge Sn

- Graphene, silicene, germanene, tinene?
- Spin orbit interactions become drastically larger as increasing atomic number

	t(eV)	$v_F(10^5\mathrm{m/s})$	a(Å)	λ_{SO}(meV)	λ_{R2}	ℓ	θ
Graphene	2.8	9.8	2.46	10^{-3}	0	0	90
Silicene	1.6	5.5	3.86	3.9	0.7	0.23	101.7
Germanene	1.3	4.6	4.02	43	10.7	0.33	106.5

- Fermi velocity smaller

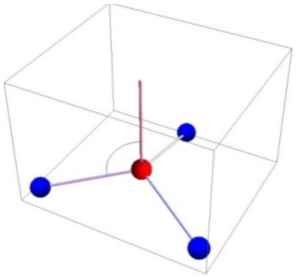

C-C, Liu, H.Jiang and Y. Yao, PRB **84** 195430 (2011)

Tight Binding Model

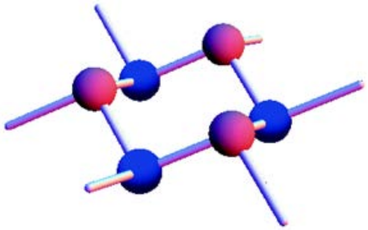

Spin-orbit term

$$H = -t \sum_{\langle i,j\rangle\alpha} c^{\dagger}_{i\alpha} c_{j\alpha} + \mathrm{i}\frac{\lambda_{\mathrm{SO}}}{3\sqrt{3}} \sum_{\langle\langle i,j\rangle\rangle\alpha\beta} \nu_{ij} c^{\dagger}_{i\alpha} \sigma^{z}_{\alpha\beta} c_{j\beta}$$

Second Rashba term

$$- i\frac{2}{3}\lambda_{\mathrm{R2}} \sum_{\langle\langle i,j\rangle\rangle\alpha\beta} \mu_i c^{\dagger}_{i\alpha} \left(\boldsymbol{\sigma} \times \hat{\boldsymbol{d}}_{ij}\right)^{z}_{\alpha\beta} c_{j\beta}$$

$t = 1.6\,\mathrm{eV}$

$\lambda_{\mathrm{SO}} = 3.9\,\mathrm{meV}$

$\lambda_{\mathrm{R}} = 0.7\,\mathrm{meV}$

$a = 3.86\,\text{Å}$

$\ell = 0.23\,\text{Å}$

$$\nu_{ij} = (\boldsymbol{d}_i \times \boldsymbol{d}_j) / |\boldsymbol{d}_i \times \boldsymbol{d}_j|$$

+ controllable interactions

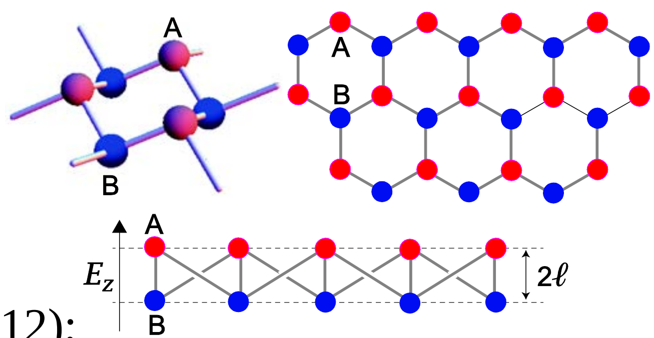

C. L. Kane and E. J. Mele, PRL 95. 226801 (2005)
C-C, Liu, H.Jiang and Y. Yao PRB **84** 195430 (2011)

M. Ezawa, NJP 14 033003 (2012); PRL 109, 055502 (2012); PRL 110, 026603 (2013); PRB 87, 155415 (2013)

Dirac Theory of Silicene

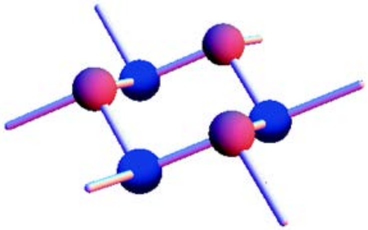

- Low-energy dynamics of silicene is described by the Dirac theory as in graphene:

$$H_\eta = \hbar v_{\mathrm{F}} \left(\eta k_x \tau_x + k_y \tau_y\right) + \eta \tau_z \lambda_{\mathrm{SO}} \sigma_z$$
$$+ \eta \tau_z a \lambda_{\mathrm{R2}} \left(k_y \sigma_x - k_x \sigma_y\right)$$
$$+ \text{controllable interactions}$$

$$v_{\mathrm{F}} = \frac{\sqrt{3}}{2} a t = 5.5 \times 10^5 \mathrm{m/s}$$

- Possible interactions are of the form:

$$H_{pqr} = \lambda_{pqr} \eta^p (\sigma_z)^q (\tau_z)^r$$

- The Dirac mass:

$$\Delta^\eta_{s_z} = \eta s_z \lambda_{\mathrm{SO}} - \ell E_z + \eta \lambda_\Omega + s_z \Delta M$$

$\lambda_{111} = \lambda_{\mathrm{SO}}$	SO interaction
$\lambda_{001} = -\ell E_z$	Electric field
$\lambda_{101} = \lambda_\Omega$	Photo-irradiation
$\lambda_{011} = \Delta M$	Exchange fields

M. Ezawa, NJP 14 033003 (2012); PRL 109, 055502 (2012); PRL 110, 026603 (2013); PRB 87, 155415 (2013)

Tight Binding Model (2)

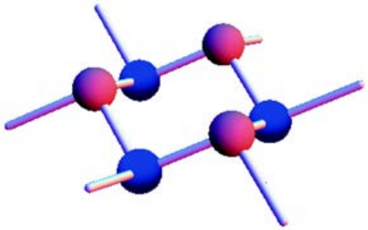

$$H = -t\sum_{\langle i,j\rangle\alpha} c_{i\alpha}^{\dagger}c_{j\alpha} + \mathrm{i}\frac{\lambda_{\mathrm{SO}}}{3\sqrt{3}}\sum_{\langle\langle i,j\rangle\rangle\alpha\beta}\nu_{ij}c_{i\alpha}^{\dagger}\sigma_{\alpha\beta}^{z}c_{j\beta}$$

Spin-orbit term

$$-i\frac{2}{3}\lambda_{\mathrm{R2}}\sum_{\langle\langle i,j\rangle\rangle\alpha\beta}\mu_i c_{i\alpha}^{\dagger}\left(\boldsymbol{\sigma}\times\hat{\boldsymbol{d}}_{ij}\right)_{\alpha\beta}^{z}c_{j\beta}$$

Second Rashba term

$$-\ell\sum_{i\alpha} t_z^i E_z c_{i\alpha}^{\dagger}c_{i\alpha} + i\frac{\lambda_{\Omega}}{3\sqrt{3}}\sum_{\langle\langle i,j\rangle\rangle\alpha\beta}\nu_{ij}c_{i\alpha}^{\dagger}c_{j\beta}$$

Electric field

Photo-irradiation

$$+\sum_{i\alpha} M_{t_z^i}c_{i\alpha}^{\dagger}\sigma_z c_{i\alpha} \Longrightarrow \Delta M\sigma_z\tau_z + \overline{M}\sigma$$

Exchange field

$$\overline{M} = (M_A + M_B)/2,$$

$$\Delta M = (M_A - M_B)/2$$

M. Ezawa, NJP 14 033003 (2012); PRL 109, 055502 (2012); PRL 110, 026603 (2013); PRB 87, 155415 (2013)

Controllable Gap of Silicene

- The simplest example with the use of the electric field E_z

$$H_\eta = \begin{pmatrix} \eta s_z \lambda_{SO} - \ell E_z & \eta k_x - i k_y \\ \eta k_x + i k_y & -(\eta s_z \lambda_{SO} - \ell E_z) \end{pmatrix}$$

$$E = \pm\sqrt{k^2 + (\eta s_z \lambda_{SO} - \ell E_z)^2}$$

$$\Delta(E_z) = 2\left|\ell E_z - \eta s_z \lambda_{SO}\right|$$

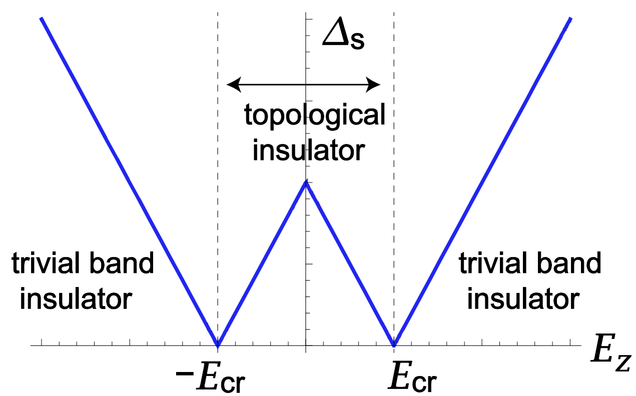

$$E_c = \lambda_{SO}/\ell = 17\mathrm{meV/Å}.$$

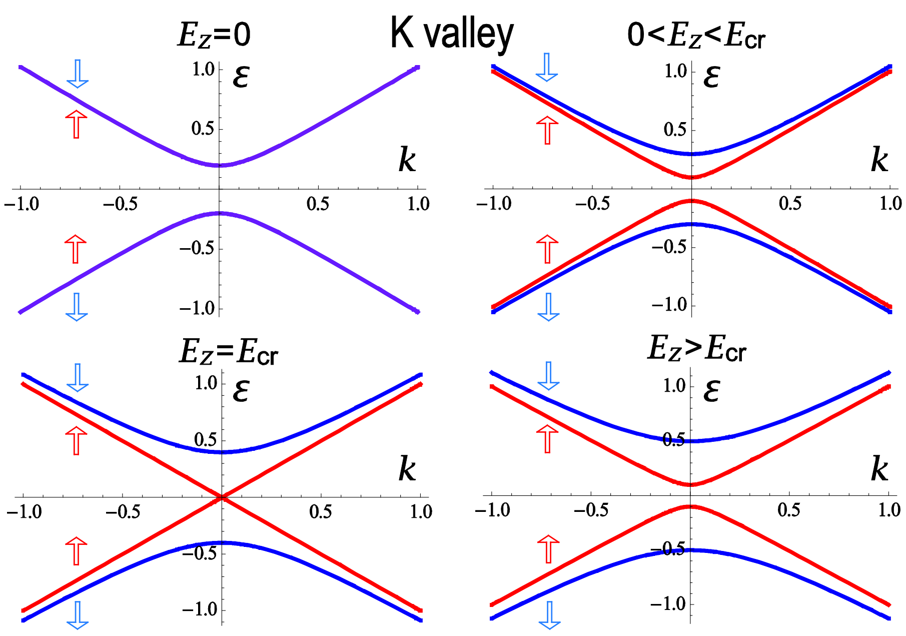

The gap closes at the critical electric field Ecr

M.Ezawa, NJP 14 033003 (2012)

Bulk-Edge Correspondence

Bulk-edge correspondence gives
an excellent signal of a topological insulator

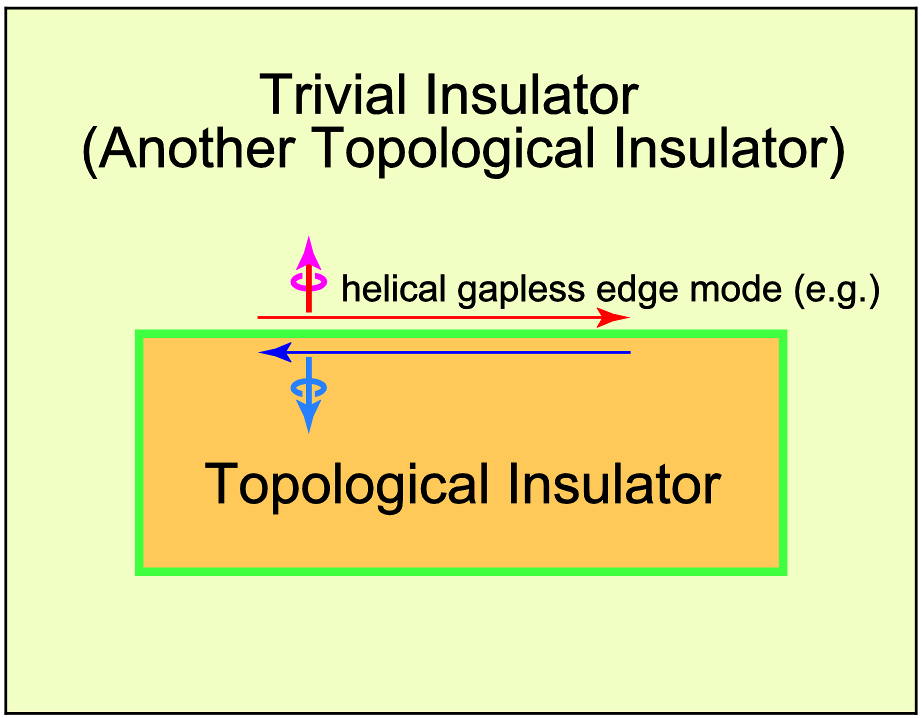

- Gapless edge modes emerge along the phase boundary between two different topological insulators
- They are topologically protected
- Each gapless mode provides one conduction channel along the edge

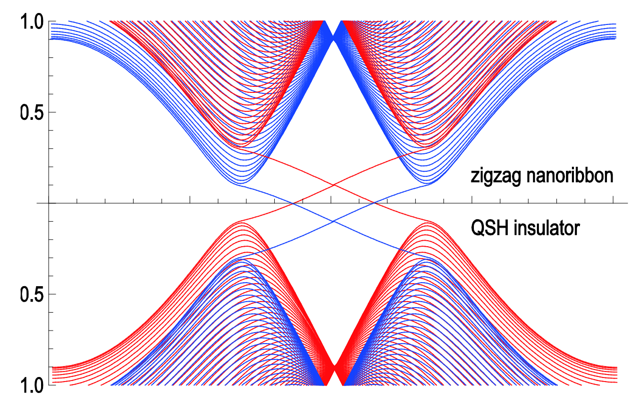

Zigzag and armchair edge

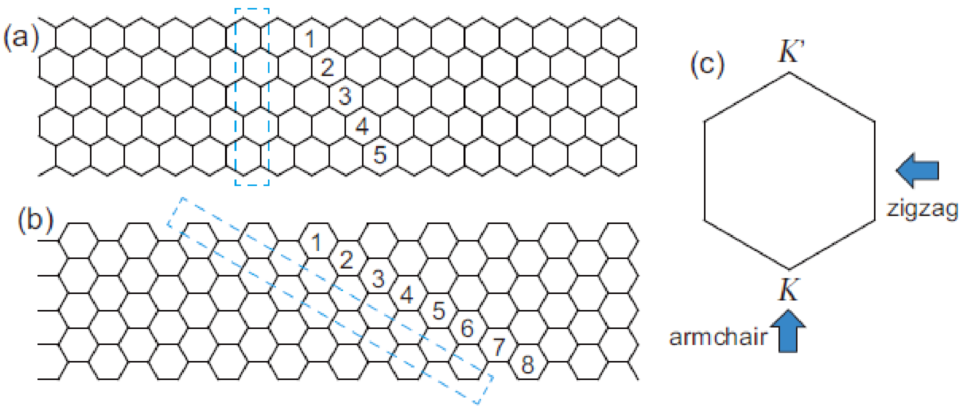

$$H = \sigma_z \tau_z^{\mathrm{edge}} \lambda_{\mathrm{SO}} \hbar v_{\mathrm{F}} k_x / t,$$

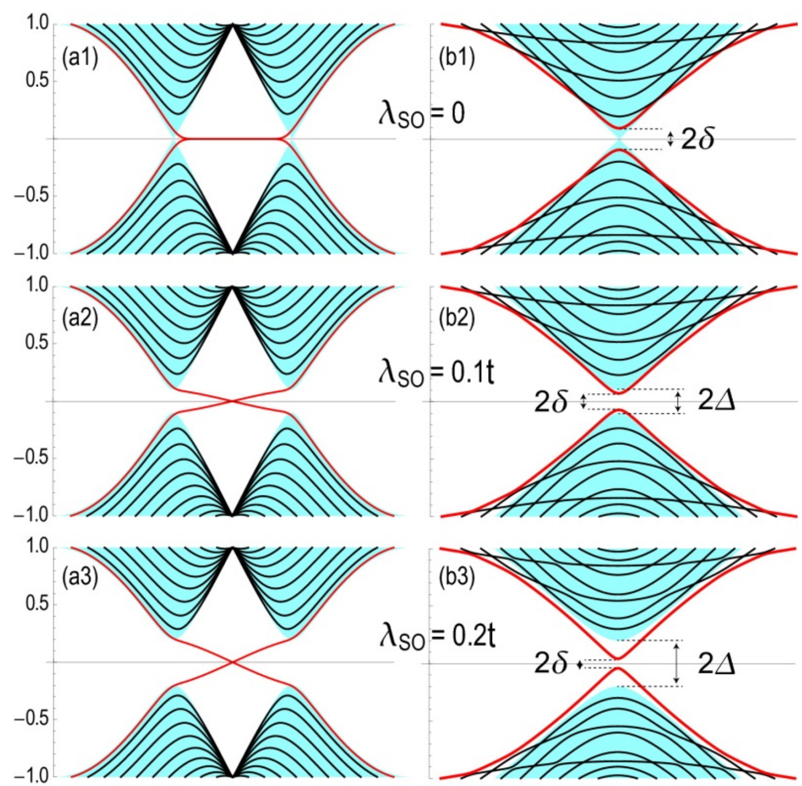

zigzag armchair

◆ Wave function of zigzag edge

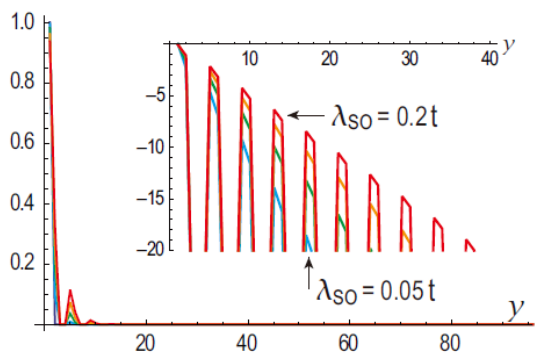

M.Ezawa and N. Nagaosa, cond-mat/arXiv.1301.6337

Emergence of Edge Modes in Armchair Edge

$$\delta \sim \Delta \exp[-W/\xi_{\mathrm{arm}}]$$

$$\xi_{\mathrm{arm}} \sim \hbar v_{\mathrm{F}}/\Delta$$

- No zero-energy states but edge modes in armchair edge
- Interference of topologically protected edge states

$$H = \sigma_z \tau_z^{\mathrm{edge}} \hbar v_{\mathrm{F}} k_x + S \tau_x^{\mathrm{edge}}$$

Band gap

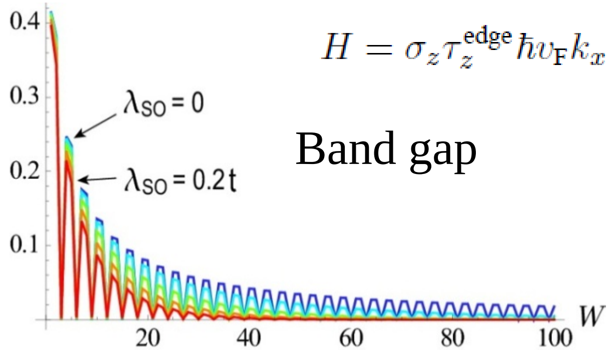

- Wave function

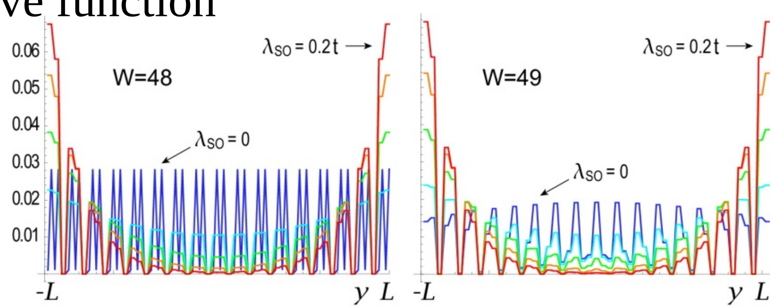

$$\psi_+(y) = (\psi_{+L}(y) + \psi_{-L}(y))/\sqrt{2} = \cosh(y/\xi_{\mathrm{arm}})$$

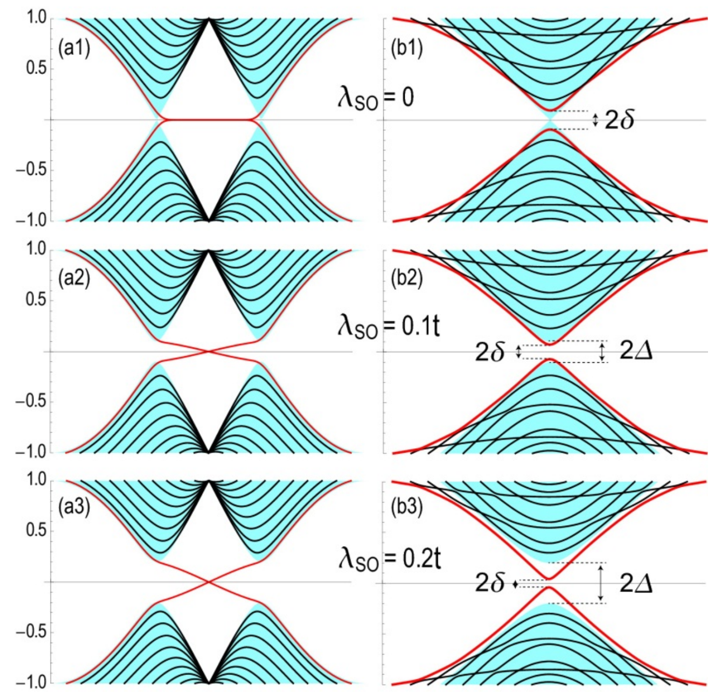

zigzag armchair

M.Ezawa and N. Nagaosa, cond-mat/arXiv.1301.6337

Quasiparticle interference

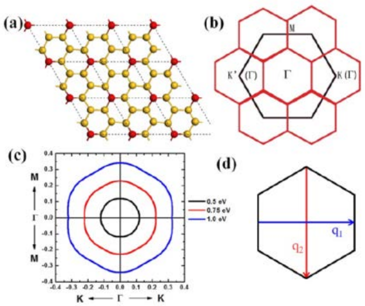

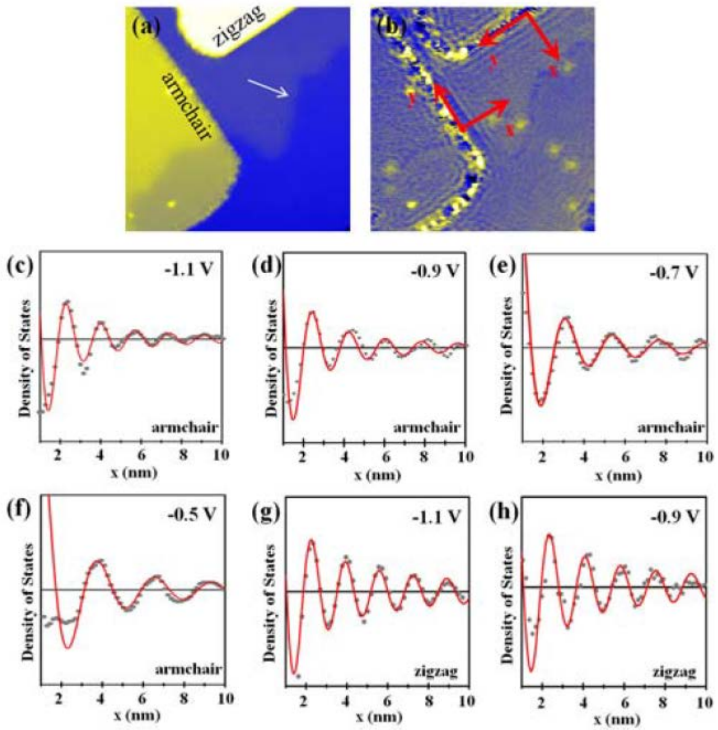

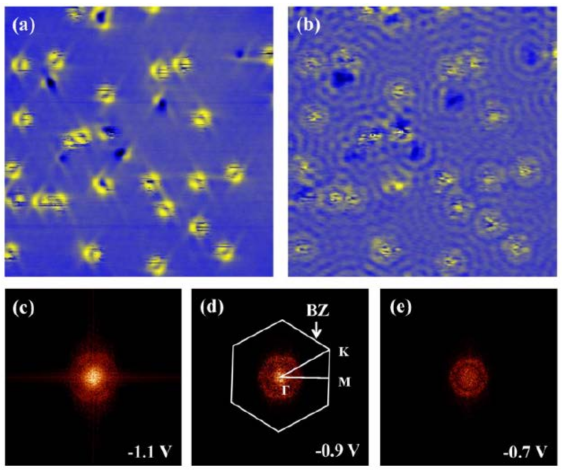

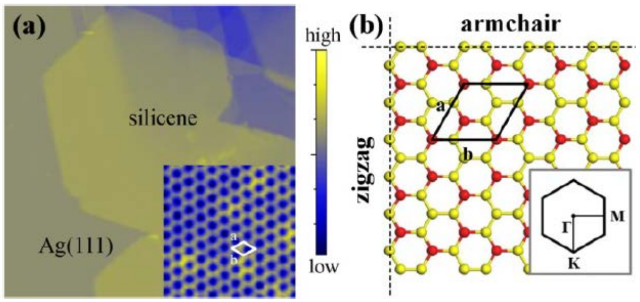

B. Feng, K. Wu et al. cond-mat/arXiv:1304.3308

DOS and Quantized Conductance

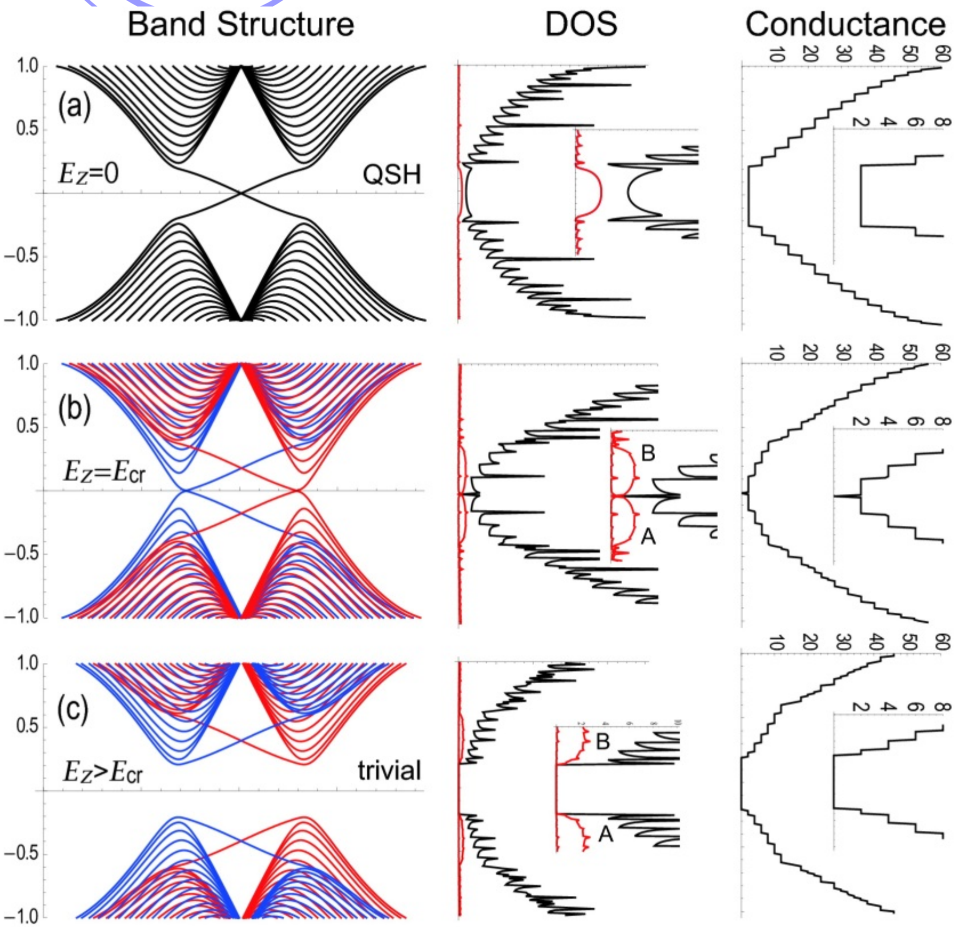

- Easiest way to observe the topological phase transition
- One quantized conductance per one channel
- Unit conductance is e^2/h
- Conductance is different in each phase
- Field-effect topological quantum transistor

topological insulator	QAH	QSH	SQAH	trivial
topological numbers	(2,0)	(0,1)	(1,1/2)	(0,0)
conductance (σ)	2	2	1	0

M.Ezawa, Appl. Phys. Lett. 102, 172103 (2013)

Topological Phase Transition

- Topological phase transition occurs when the sign of Dirac mass changes
- Dirac mass in silicene is given by

$$\Delta_{s_z}^{\eta} = \eta s_z \lambda_{\mathrm{SO}} - \ell E_z + \eta \lambda_{\Omega} + s_z \Delta M$$

- Electric field induced mass term
- Photo-induced Haldane mass term
- Antiferromagnet-induced mass term

	Order	TRS	SRS	SLS
111	Kane-Mele	True	False	False
001	CDW	True	True	False
011	AF	False	False	False
101	Haldane	False	True	False

M. Ezawa, PRB 87, 155415 (2013)

Chern and Spin Chern Numbers

- Spin Chern number(Mod2) = Z_2 index, when s_z is conserved
- They are determined by the Dirac mass

$$\mathcal{C}^{\eta}_{s_z} = \frac{1}{4\pi}\int d^2k \left(\frac{\partial \hat{\mathbf{d}}}{\partial k_x} \times \frac{\partial \hat{\mathbf{d}}}{\partial k_y}\right)\cdot \hat{\mathbf{d}}$$

Pontryagin number

$$\mathcal{C}^{\eta}_{s_z} = \frac{\eta}{4\pi}\int d^2k\ \varepsilon_{ij}\partial_i\sigma\partial_j\theta = \frac{\eta}{2}\int_0^1 d\sigma = \frac{\eta}{2}\mathrm{sgn}(\Delta^{\eta}_{s_z})$$

$$\sigma(k) = \frac{\Delta^{\eta}_{s_z}}{\sqrt{(\hbar v_{\mathrm{F}} k)^2 + (\Delta^{\eta}_{s_z})^2}}$$

$$H_\eta = \begin{pmatrix} \Delta^{\eta}_{s_z} & \hbar v_{\mathrm{F}}(\eta k_x - i k_y) \\ \hbar v_{\mathrm{F}}(\eta k_x + i k_y) & -\Delta^{\eta}_{s_z} \end{pmatrix}$$

$$H = \boldsymbol{\tau}\cdot\mathbf{d}$$

$$d_x = \eta\hbar v_{\mathrm{F}} k_x,\quad d_y = \hbar v_{\mathrm{F}} k_y,\quad d_z = \Delta^{\eta}_{s_z}$$

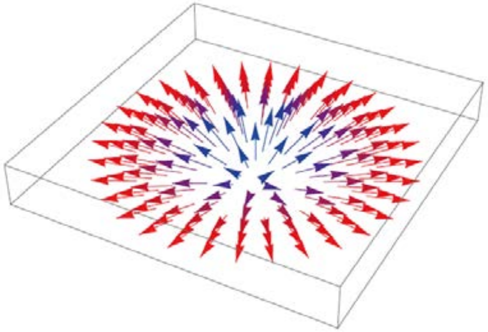

Meron pseudospin texture

M.Ezawa, Euro. Phys. J. B 85, 363 (2012)

Classification of Topological Insulators

$\mathcal{C}_\uparrow^K$	$\mathcal{C}_\uparrow^{K'}$	$\mathcal{C}_\downarrow^K$	$\mathcal{C}_\downarrow^{K'}$	$\mathcal{C}$	$2\mathcal{C}_s$	$\mathcal{C}_v$	$\mathcal{C}_{sv}$	
$1/2$	$1/2$	$1/2$	$1/2$	2	0	0	0	QAH
$1/2$	$1/2$	$1/2$	$-1/2$	1	1	1	-1	SQAH
$1/2$	$1/2$	$-1/2$	$1/2$	1	-1	1	1	SQAH
$1/2$	$1/2$	$-1/2$	$-1/2$	0	0	2	0	CDW
$1/2$	$-1/2$	$1/2$	$1/2$	1	1	-1	1	SQAH
$1/2$	$-1/2$	$1/2$	$-1/2$	0	2	0	0	QSH
$1/2$	$-1/2$	$-1/2$	$1/2$	0	0	0	2	AF
$1/2$	$-1/2$	$-1/2$	$-1/2$	-1	1	1	1	SQAH
$-1/2$	$1/2$	$1/2$	$1/2$	1	-1	-1	-1	SQAH
$-1/2$	$1/2$	$1/2$	$-1/2$	0	0	0	-2	AF
$-1/2$	$1/2$	$-1/2$	$1/2$	0	-2	0	0	QSH
$-1/2$	$1/2$	$-1/2$	$-1/2$	-1	-1	1	-1	SQAH
$-1/2$	$-1/2$	$1/2$	$1/2$	0	0	-2	0	CDW
$-1/2$	$-1/2$	$1/2$	$-1/2$	-1	1	-1	-1	SQAH
$-1/2$	$-1/2$	$-1/2$	$1/2$	-1	-1	-1	1	SQAH
$-1/2$	$-1/2$	$-1/2$	$-1/2$	-2	0	0	0	QAH

Chern number

$$\mathcal{C} = \mathcal{C}_\uparrow^K + \mathcal{C}_\uparrow^{K'} + \mathcal{C}_\downarrow^K + \mathcal{C}_\downarrow^{K'}$$

Spin-Chern number

$$\mathcal{C}_s = \frac{1}{2}(\mathcal{C}_\uparrow^K + \mathcal{C}_\uparrow^{K'} - \mathcal{C}_\downarrow^K - \mathcal{C}_\downarrow^{K'})$$

Valley-Chern number

$$\mathcal{C}_v = (\mathcal{C}_\uparrow^K - \mathcal{C}_\uparrow^{K'} + \mathcal{C}_\downarrow^K - \mathcal{C}_\downarrow^{K'})$$

Spin-Valley Chern number

$$\mathcal{C}_{sv} = \frac{1}{2}(\mathcal{C}_\uparrow^K - \mathcal{C}_\uparrow^{K'} - \mathcal{C}_\downarrow^K + \mathcal{C}_\downarrow^{K'})$$

F. Zhang, J. Jung, G.A. Fiete, Q. Niu, and A.H. MacDonald PRL 106, 156801 (2011)

M. Ezawa, Phys. Rev. B 87, 155415 (2013)

Silicene with Exchange Interaction

$$\sum_{i\alpha} M_{t_z^i} c_{i\alpha}^{\dagger} \sigma_z c_{i\alpha} \Longrightarrow \Delta M \sigma_z \tau_z + \overline{M} \sigma$$

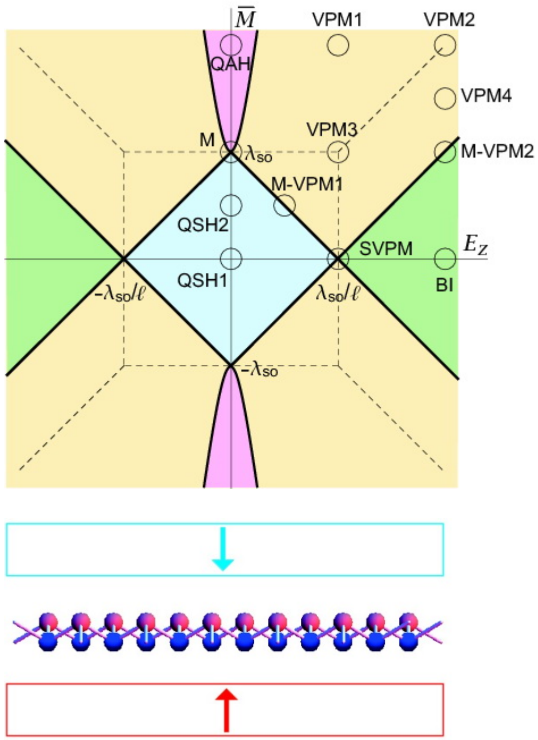

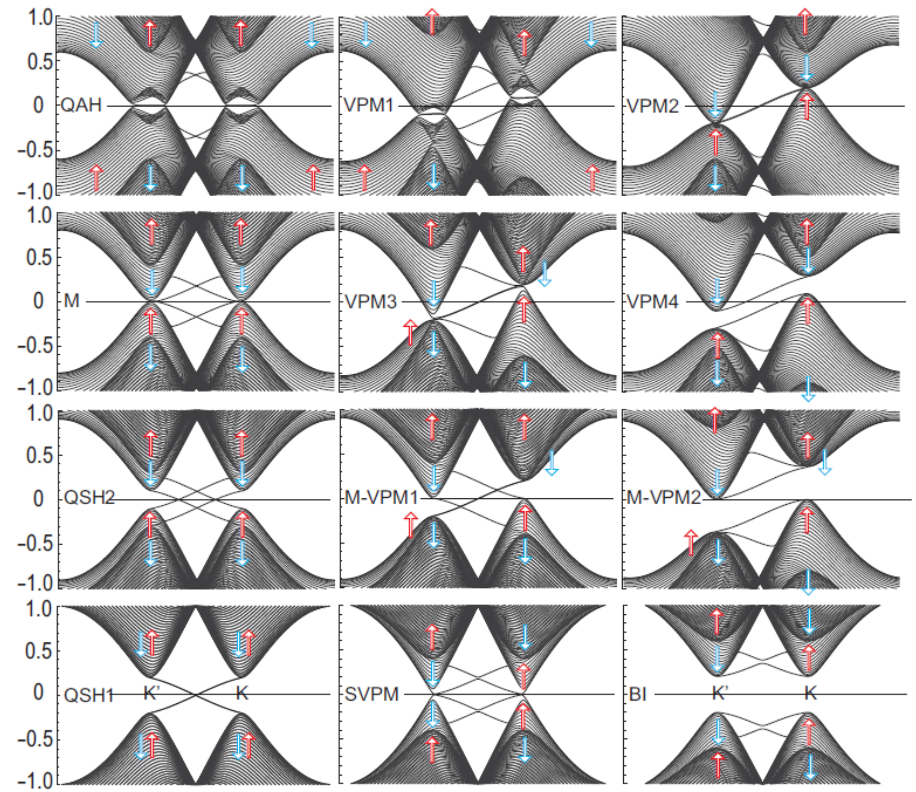

M. Ezawa, PRL 109, 055502 (2012)

W.K. Tse Z. Qiao, Y. Yao, A. H. MacDonald, and Qian Niu, PRB 83, (2011) 155447.

Quantum Anomalous Hall Effect

- QAHE is QHE without magnetic field (nonzero Chern number)
- The QAH phase has flat gapless edge modes

Excange field $M \sum_{i\alpha} c_{i\alpha}^{\dagger} \sigma_z c_{i\alpha}$

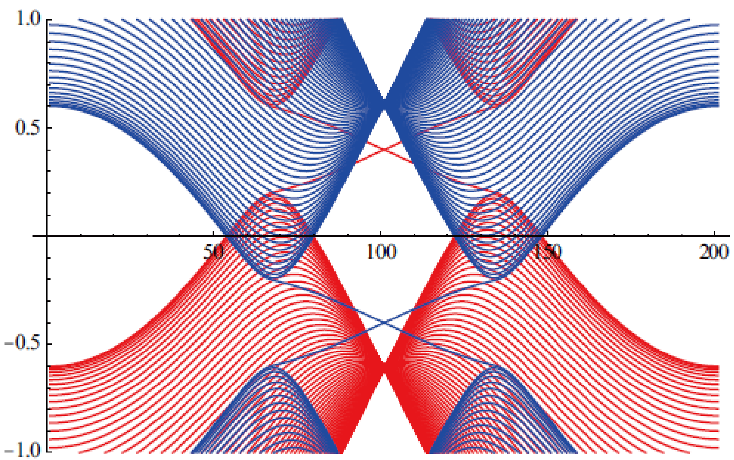

Without Rashba interaction

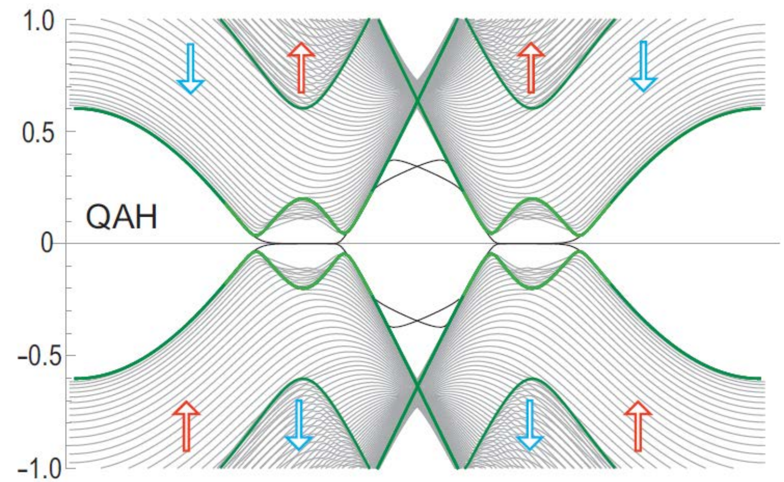

With Rashba interaction

M. Ezawa, PRL 109, 055502 (2012)

Momentum Space Skyrmion

- Spins form a momentum-space skyrmion to yield the Chern number

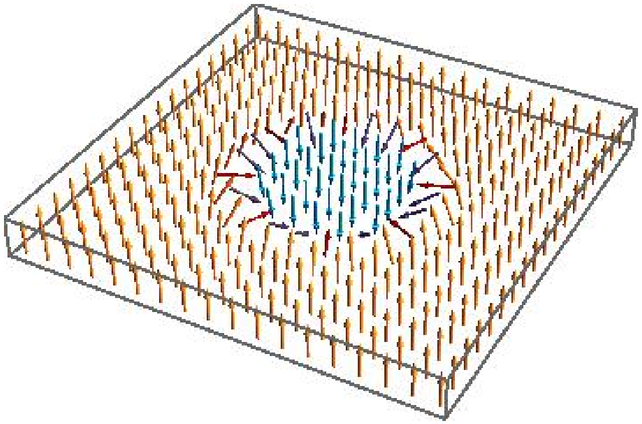

Skyrmion spin texture

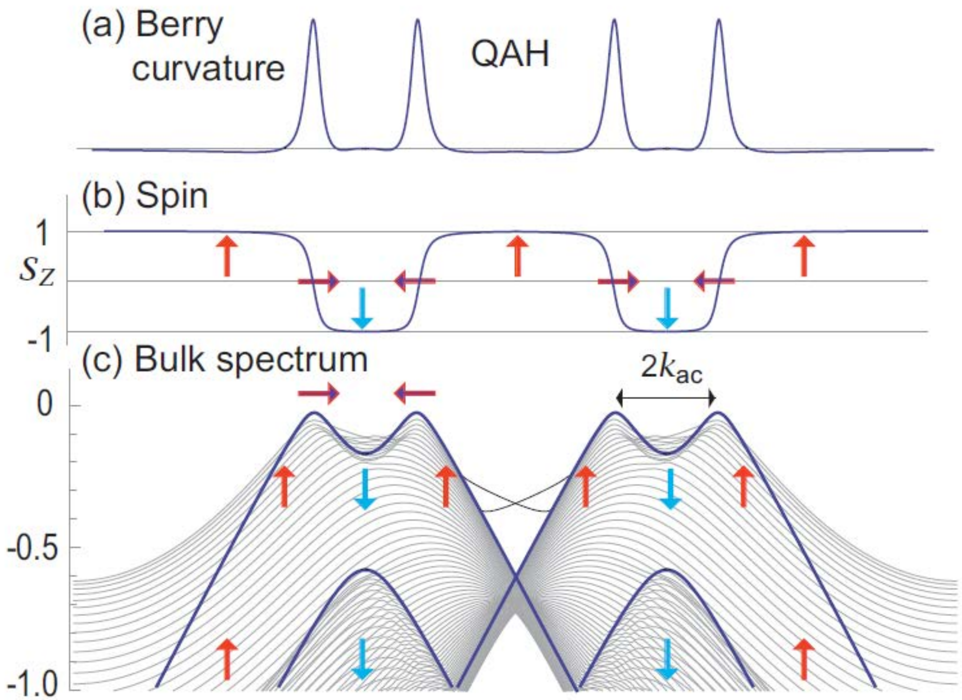

M. Ezawa, PRL 109, 055502 (2012)

Valley Polarized Metal

Valley polarization

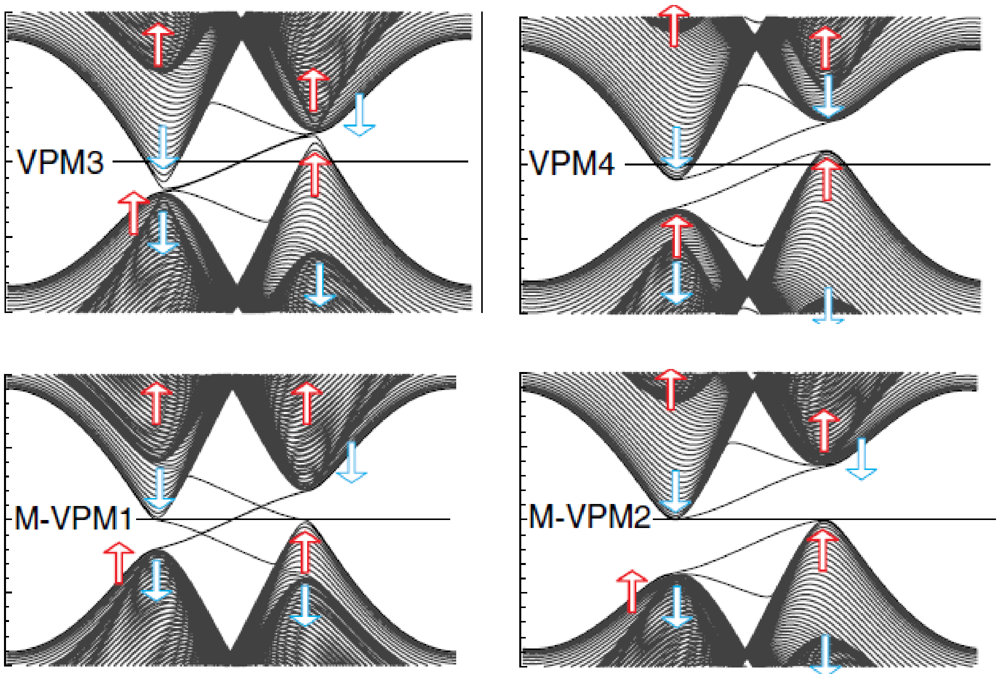

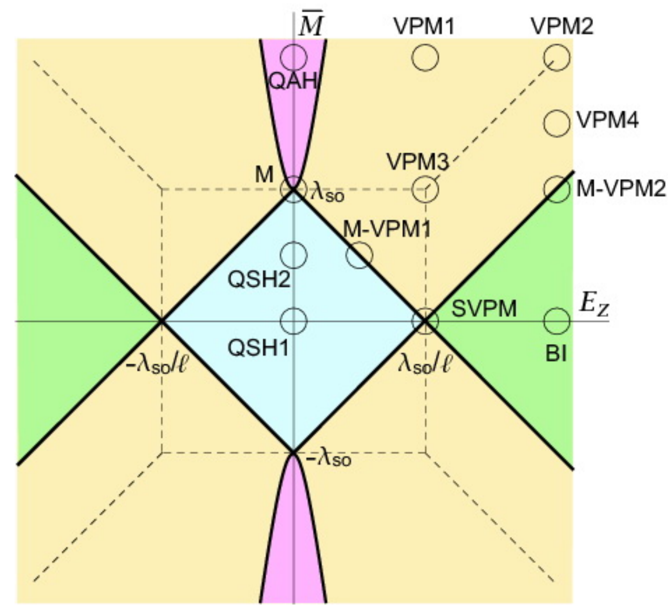

M. Ezawa, PRL 109, 055502 (2012)

Antiferromagnet and Electric Fields

$$H_\eta = \hbar v_{\mathrm{F}} \left(\eta k_x \tau_x + k_y \tau_y\right) + \eta \sigma_z \tau_z \lambda_{\mathrm{SO}} - \ell E_z \tau_z$$
$$+ \eta \tau_z a \lambda_{\mathrm{R2}} \left(k_y \sigma_x - k_x \sigma_y\right) + \overline{M} \sigma_z + \Delta M \sigma_z \tau_z$$

$$\overline{M} = \tfrac{1}{2}(M_A + M_B) \text{ and } \Delta M = \tfrac{1}{2}(M_A - M_B)$$

$$\Delta_{s_z}^{\eta} = \eta s_z \lambda_{\mathrm{SO}} + s_z \Delta M - \ell E_z$$

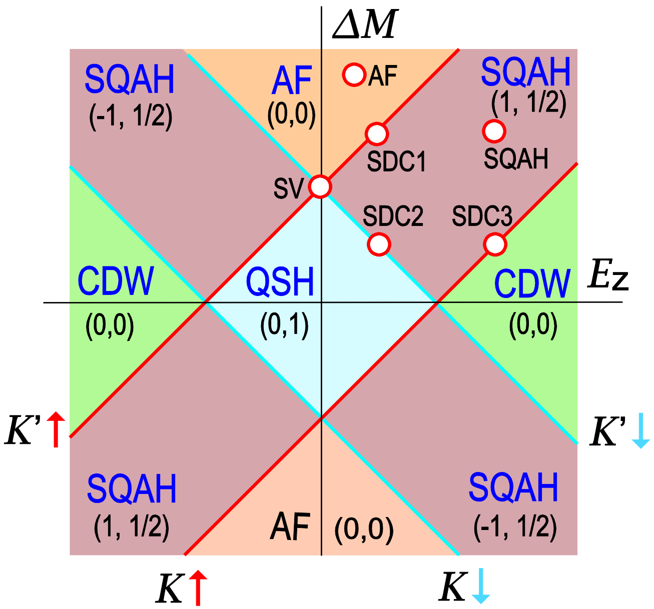

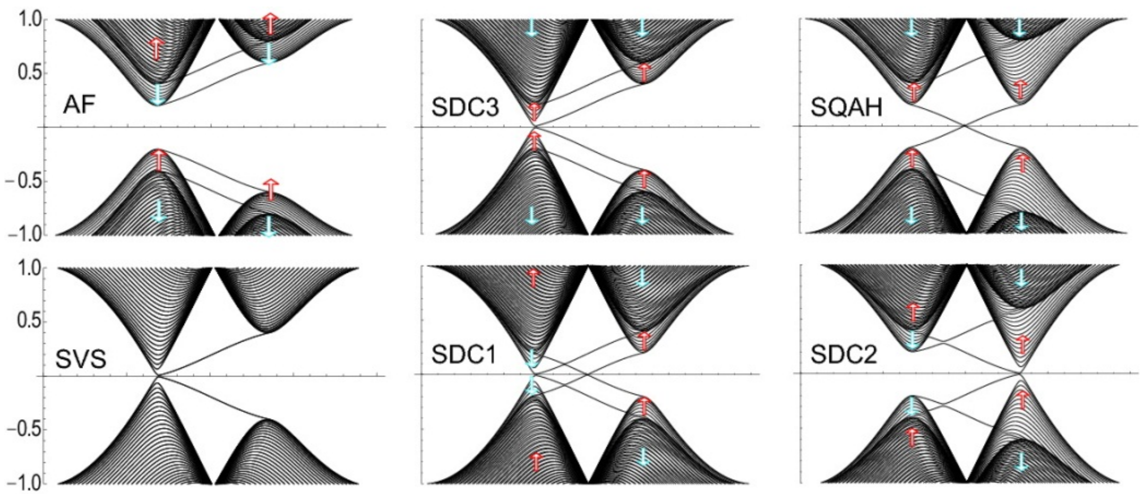

M. Ezawa, PRB 87, 155415 (2013)

QHE with High Spin-Chern Number

$$E_N = \pm\sqrt{(\hbar\omega_c)^2 N + (\Delta^{\eta}_{s_z})^2}, \quad N = 1, 2, \cdots,$$

Dirac theory

Hofstadter’s butterfly

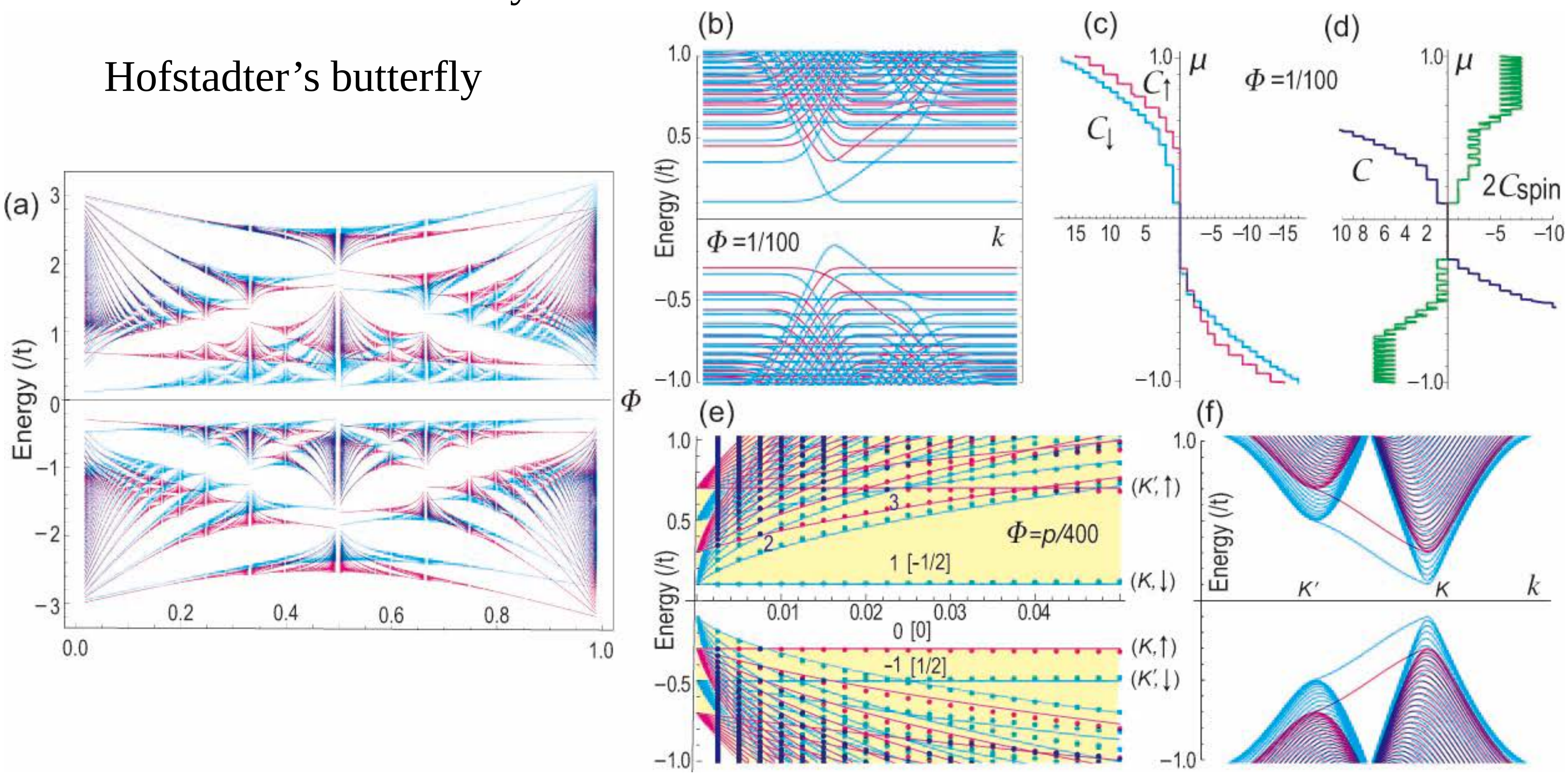

M. Ezawa, cond-mat/1306.1859

Fan diagram

QSQAHE and Single Valley Semimetal

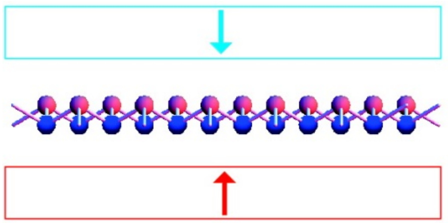

Due to the silicene's buckled structure, different exchange fields *MA* and *MB* operate on the *A* and *B* sites

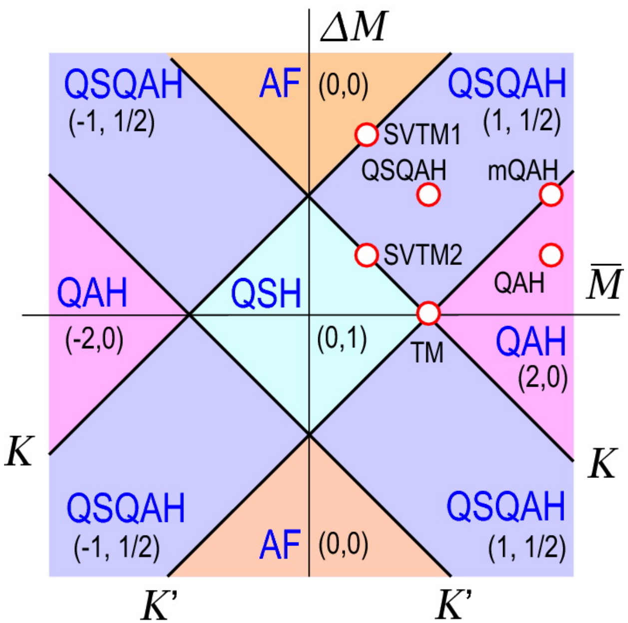

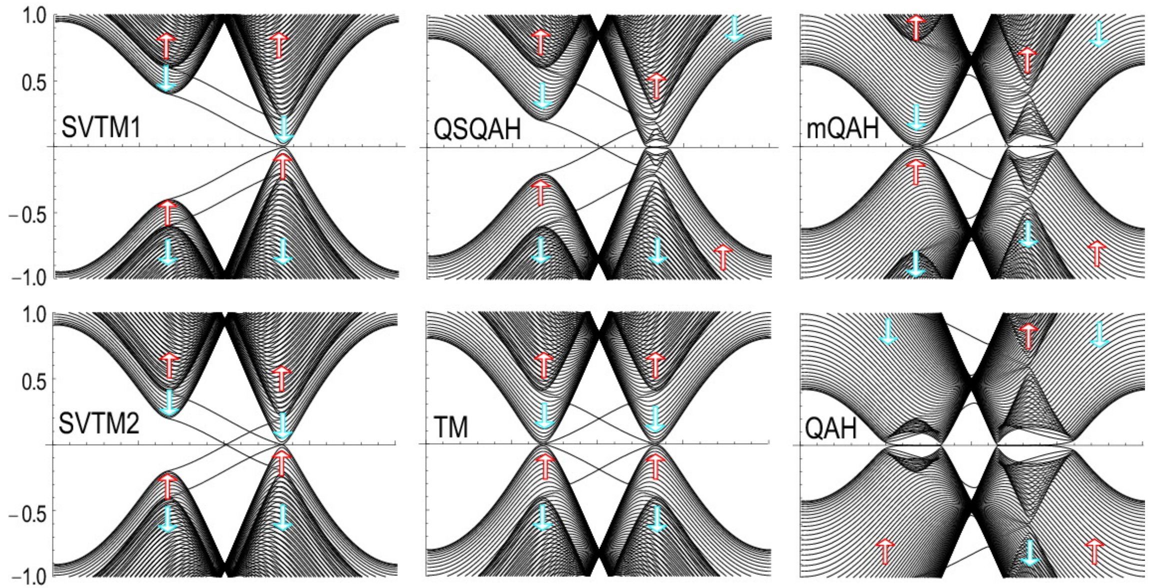

$$\mathcal{C}^{K} = \frac{1}{2}\text{sgn}\left(\lambda_{\text{SO}} + M_{A}\right) + \frac{1}{2}\text{sgn}\left(-\lambda_{\text{SO}} + M_{B}\right)$$

$$\mathcal{C}^{K'} = \frac{1}{2}\text{sgn}\left(-\lambda_{\text{SO}} + M_{A}\right) + \frac{1}{2}\text{sgn}\left(\lambda_{\text{SO}} + M_{B}\right)$$

M. Ezawa, PRB 87, 155415 (2013)

Photo-Induced Topological Phase Transition

Circular polarized light

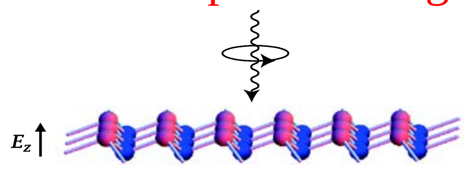

Floquet theory

Photoinduced Haldane term

Off resonance condition

$\hbar|\Omega| \gg t$ 100THz

$$\Delta H_{\text{eff}} = i\eta\hbar v_{\text{F}}^2 \mathcal{A}^2/(3\sqrt{3}\Omega) \sum_{\langle\langle i,j\rangle\rangle\alpha\beta} \nu_{ij} c_{i\alpha}^{\dagger} c_{j\beta}.$$

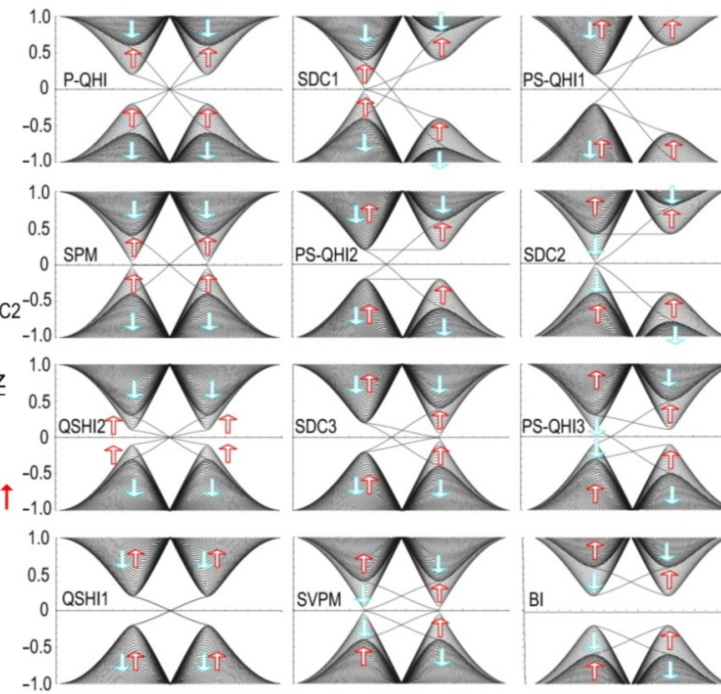

$$\Delta H_{\text{eff}} = -\frac{\mathcal{A}^2}{\hbar\Omega}\left[(\hbar v_{\text{F}})^2 \eta\tau_z - (a\lambda_{\text{R2}})^2 \sigma_z - a\lambda_{\text{R2}}\hbar v_{\text{F}}(\eta\tau_x\sigma_y - \tau_y\sigma_x)\right]$$

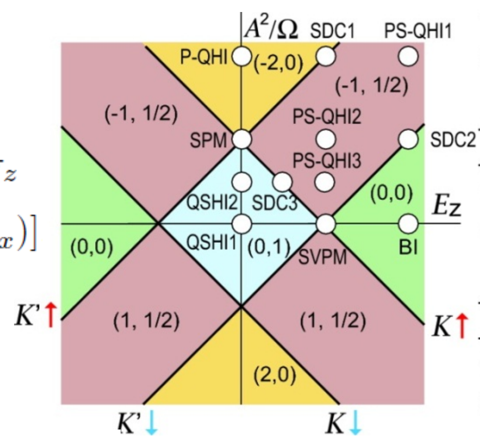

Dirac mass

$$m_{\text{D}} = -s_z t_z \lambda_{\text{SO}} + \ell E_z - \eta\hbar v_{\text{F}}^2 \mathcal{A}^2\Omega^{-1}$$

M. Ezawa, PRL**110**, 026603 (2013)

Topological Semimetal and Topological Metal

- Two types of topological phase transitions
- One occurs when the Dirac mass becomes zero,
  (electric field, photo-irradiation, antiferromagnet)

$$\Delta_{s_z}^{\eta} = \eta s_z \lambda_{SO} - \ell E_z + \eta \lambda_\Omega + s_z \Delta M.$$

- Other occurs when the band edge touches the Fermi energy (ferromagnet)
- Provided it is sandwiched by two different topological insulators,
  a topological semimetal or metal emerge along the phase boundary

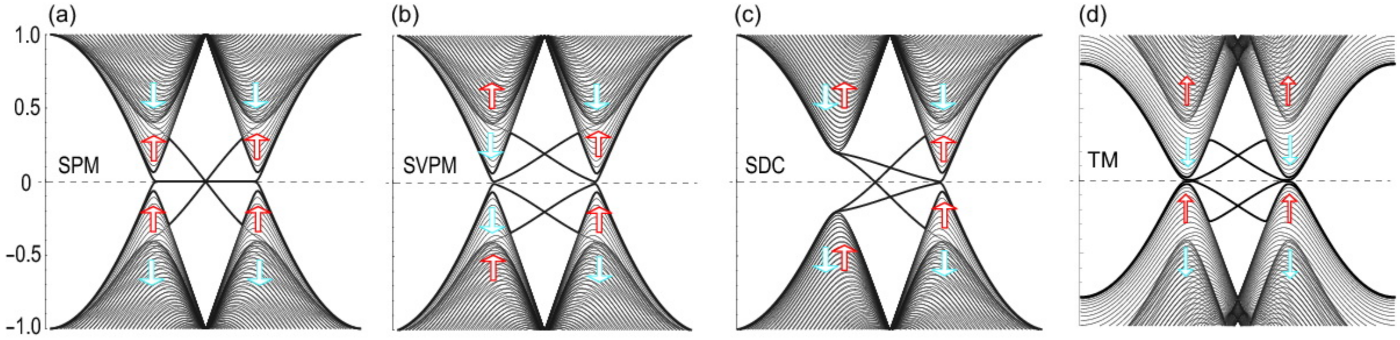

M. Ezawa, PRB 87, 155415 (2013)

Silicene Derivatives

Silicon nanotube

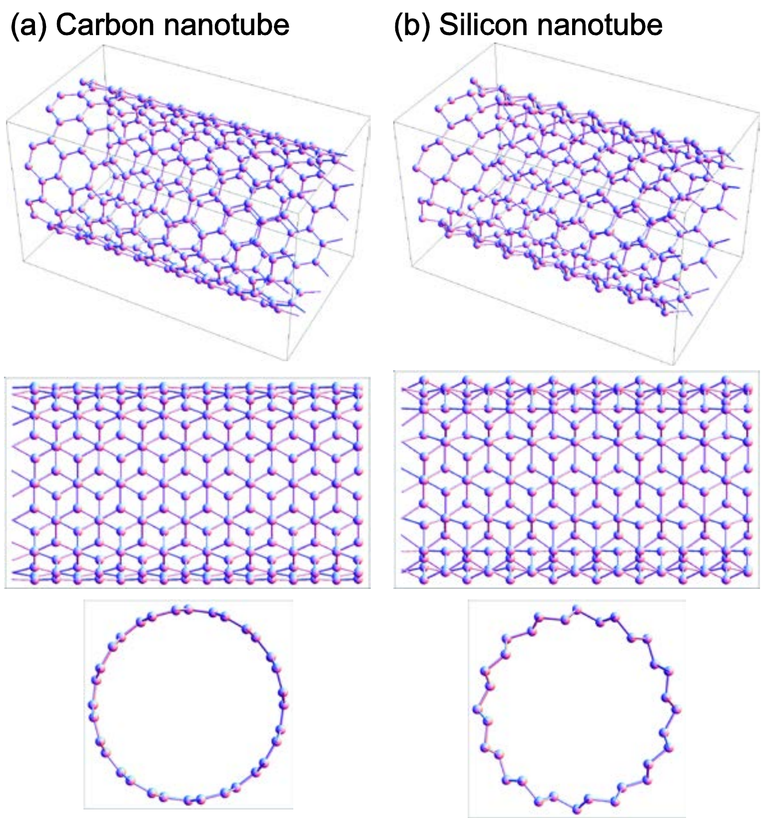

Bilayer silicene

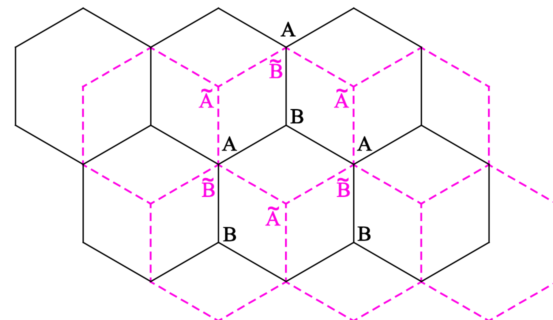

Multilayer silicene
Silicite? (Graphite made of silicon)
Silicon fullerenes

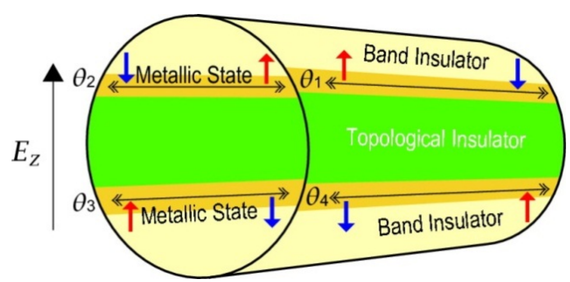

M.Ezawa, Eur. Phys. J. B 85, 363 (2012)

Conclusion

- Silicene is a graphene-like silicon honeycome structure
- The band gap can be tuned by external electric field
- Topologically protected zero-energy edge channels transport quantized conductance → topological quantum nanodevices
- Many new topological phases emerge in silicen

★ *QAH with flat chiral edge and momentum skyrmion*

★*QAHE with anisotropic chiral edge*

★ *Single Dirac Cone State*, ★ *Spin-Polarized QHE*

★ *Hybrid Topological Insulator*, ★ *Single-Valley Semimetal*

★ *Topological Semimetal and Topological Metal*

Quantum Anomalous Hall Effects in Graphene

QAH is QH without magnetic field (nonzero Chern number)

Rashba type-I

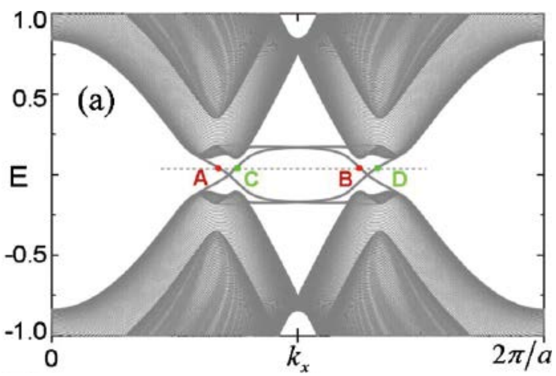

Rashba type-II

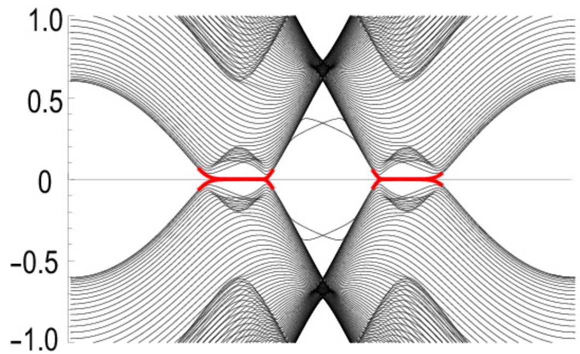

Exchange field

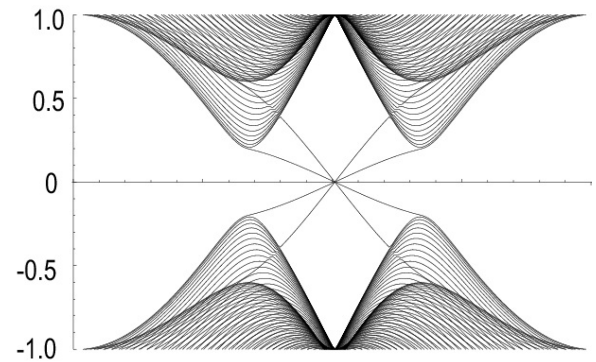

Z. Qiao, S. A. Yang, W. Feng, W.-K. Tse, J. Ding, Y. Yao, J. Wang, and Q. Niu
PRB **82**, 161414R (2010)

W.-K. Tse, Z. Qiao, Y. Yao, A. H. MacDonald, and Q. Niu, PRB **83**, 155447 (2011)

Z. Qiao, H. Jiang, X. Li, Y. Yao, and Q. Niu, PRB 85, 115439 (2012)

M. Ezawa, PRL 109, 055502 (2012); PRL110, 026603 (2013)

3x3 Si-Superstructure

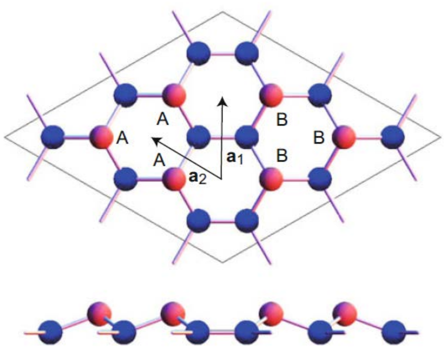

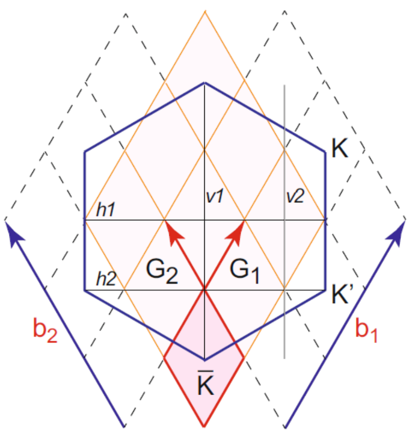

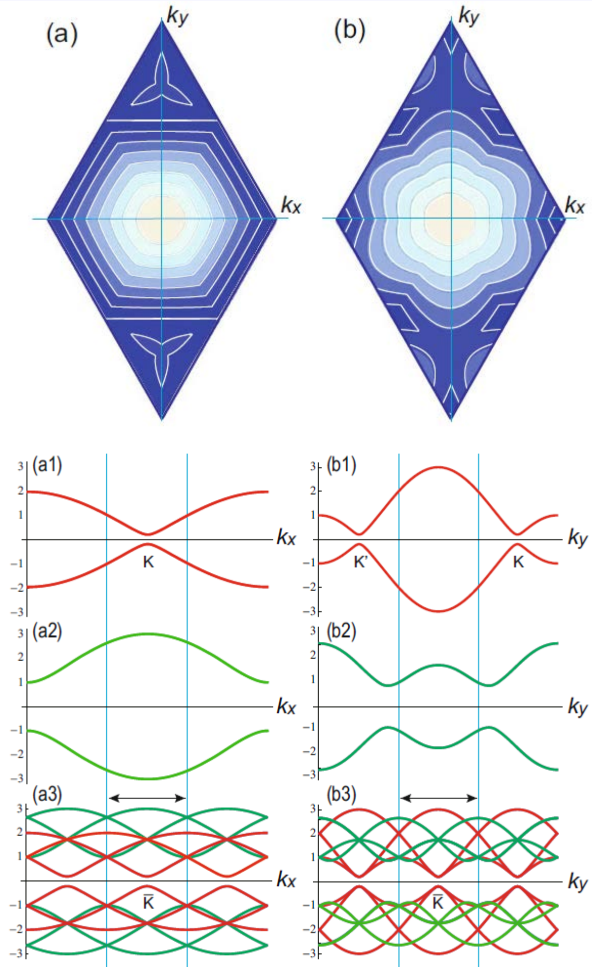

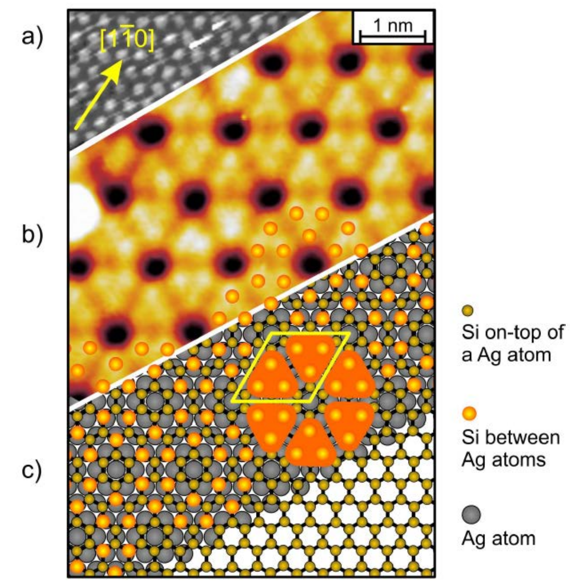

M. Ezawa, Euro. Phys. J. B 86, 139 (2013)

Various Superstructures

Ag 145 pm
Si 111 pm
145/111=1.31

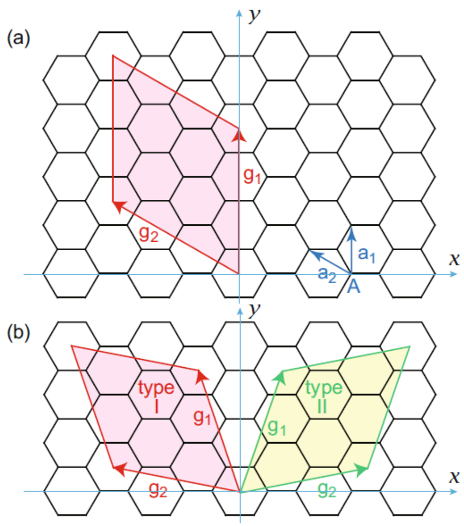

Ag-superstructure	Si-superstructure	p	q	ratio
4×4[1, 2]	3×3	3	0	1.33
$\sqrt{7} \times \sqrt{7}$	2×2	2	0	1.32
$\sqrt{13} \times \sqrt{13}$[2]	$\sqrt{7} \times \sqrt{7}$	2	1	1.36
$\sqrt{21} \times \sqrt{21}$	$2\sqrt{3} \times 2\sqrt{3}$	2	2	1.32
$2\sqrt{3} \times 2\sqrt{3}$[17]	$\sqrt{7} \times \sqrt{7}$	2	1	1.31
(free-standing)	1×1	1	0	
nothing	$\sqrt{3} \times \sqrt{3}$	1	1	

$$\tan\phi = \sqrt{3}q/(2p+q)$$

$$|\boldsymbol{g}_1| = \sqrt{p^2+q^2+pq}$$

$$N = 2\,|\boldsymbol{g}_1|^2 = 2\left(p^2+q^2+pq\right)$$

$$\boldsymbol{g}_1 = p\boldsymbol{a}_1 + q\boldsymbol{a}_2$$

$$\boldsymbol{g}_2 = e^{\pm i\pi/3}\boldsymbol{g}_1$$

$$\boldsymbol{K} - \boldsymbol{K}' = n_1\boldsymbol{G}_1 + n_2\boldsymbol{G}_2$$

$$\boldsymbol{G}_i = (\boldsymbol{g}_i \times \boldsymbol{n})/\,|\boldsymbol{g}_1 \times \boldsymbol{g}_2|$$

M. Ezawa, Euro. Phys. J. B 86, 139 (2013)

Topological Insulator, Semimetal and Metal

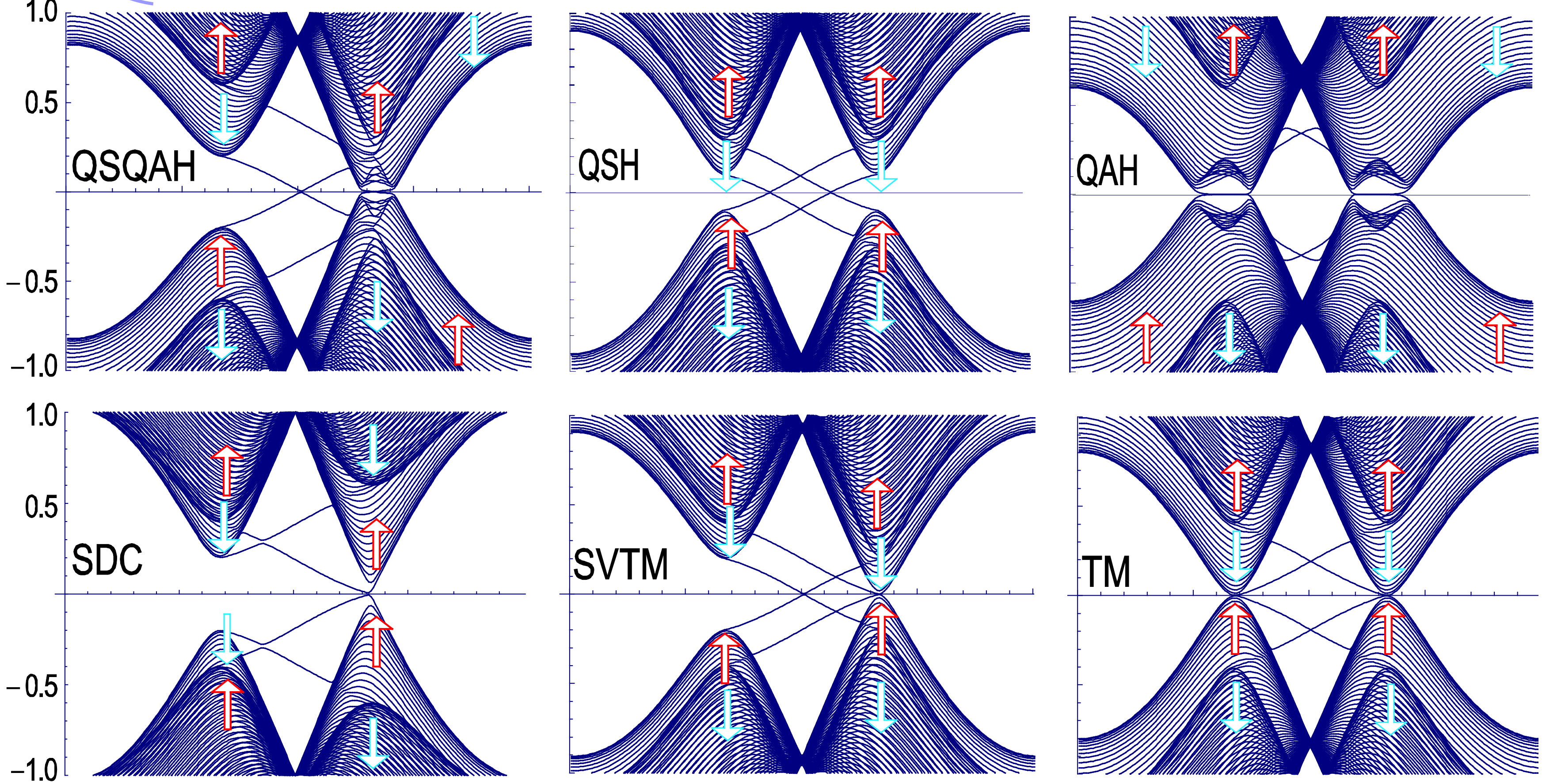

Chern and Spin Chern Numbers

- Spin Chern number(Mod2) = Z_2 index, when s_z is conserved
- They are determined by the Dirac mass

$$\mathcal{C}^{\eta}_{s_z} = \frac{1}{4\pi}\int d^2k \left(\frac{\partial \hat{\mathbf{d}}}{\partial k_x} \times \frac{\partial \hat{\mathbf{d}}}{\partial k_y}\right) \cdot \hat{\mathbf{d}}$$

Pontryagin number

$$\mathcal{C}^{\eta}_{s_z} = \frac{\eta}{4\pi}\int d^2k\, \varepsilon_{ij}\partial_i \sigma \partial_j \theta = \frac{\eta}{2}\int_0^1 d\sigma = \frac{\eta}{2}\mathrm{sgn}(\Delta^{\eta}_{s_z})$$

$$\sigma(k) = \frac{\Delta^{\eta}_{s_z}}{\sqrt{(\hbar v_{\mathrm{F}} k)^2 + (\Delta^{\eta}_{s_z})^2}}$$

$$H_\eta = \begin{pmatrix} \Delta^{\eta}_{s_z} & \hbar v_{\mathrm{F}}(\eta k_x - i k_y) \\ \hbar v_{\mathrm{F}}(\eta k_x + i k_y) & -\Delta^{\eta}_{s_z} \end{pmatrix}$$

$$H = \tau \cdot \mathbf{d}$$

$$d_x = \eta \hbar v_{\mathrm{F}} k_x, \quad d_y = \hbar v_{\mathrm{F}} k_y, \quad d_z = \Delta^{\eta}_{s_z}$$

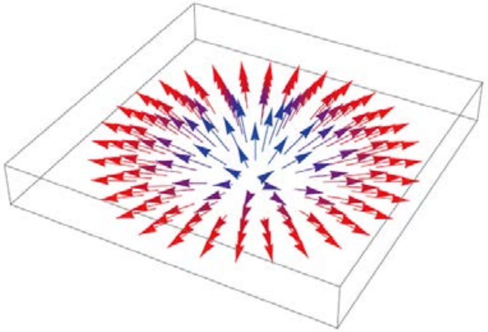

Meron pseudospin texture

M.Ezawa, Euro. Phys. J. B 85, 363 (2012)

Honeycomb AF-Dirac System

Monolayer antiferromagnetic manganese chalcogenophosphates (MnPX3, X = S, Se)
Xiao Li, Ting Cao, Qian Niu, Junren Shi, Ji Feng,
cond-mat/arXiv:1210.4623

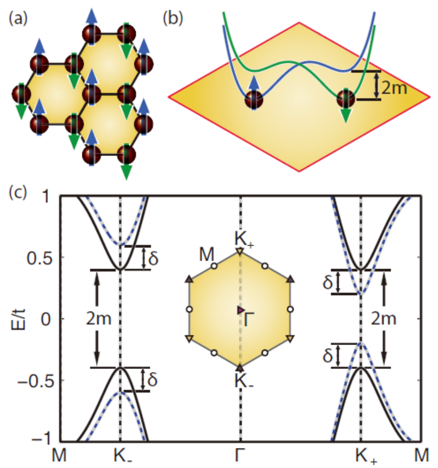

perovskite G-type antiferromagnetic insulators grown along [111] direction
Qi-Feng Liang, Long-Hua Wu, Xiao Hu,
cond-mat/arXiv:1301.4113

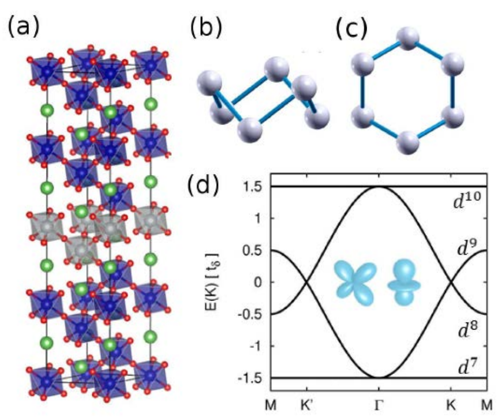

Floquet Perturbation Theory

- Effective Hamiltonian $\Delta H_{\mathrm{eff}} = (i\hbar/T)\log U$
- Time evolution operator $U = \mathcal{T}\exp[-i/\hbar \int_0^T H(t)\,dt]$
- Second order $\Delta H_{\mathrm{eff}} = (\hbar\Omega)^{-1}[H_{-1}, H_{+1}] + O(\mathcal{A}^4)$
- Floquet component $H_{\pm 1} = \frac{1}{T}\int_0^T H(T)\, e^{\pm it|\Omega|}dt$
- Haldane interaction $\Delta H_{\mathrm{eff}} = -\frac{\mathcal{A}^2}{\hbar\Omega}[(\hbar v_{\mathrm{F}})^2\, \eta\tau_z$
- Haldane term $\Delta H_{\mathrm{eff}} = i\eta\hbar v_{\mathrm{F}}^2 \mathcal{A}^2/(3\sqrt{3}\Omega) \sum_{\langle\langle i,j\rangle\rangle\alpha\beta} \nu_{ij} c_{i\alpha}^{\dagger} c_{j\beta}$
- Dirac mass $m_{\mathrm{D}} = -s_z t_z \lambda_{\mathrm{SO}} + \ell E_z - \eta\hbar v_{\mathrm{F}}^2 \mathcal{A}^2 \Omega^{-1}$

T. Kitagawa, T. Oka, A. Brataas, L. Fu, and E. Demler, Phys. Rev.B 84, 235108 (2011).

Optical Absorption of Silicene

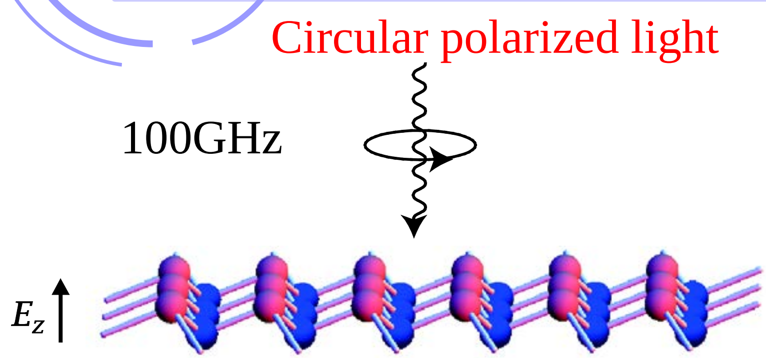

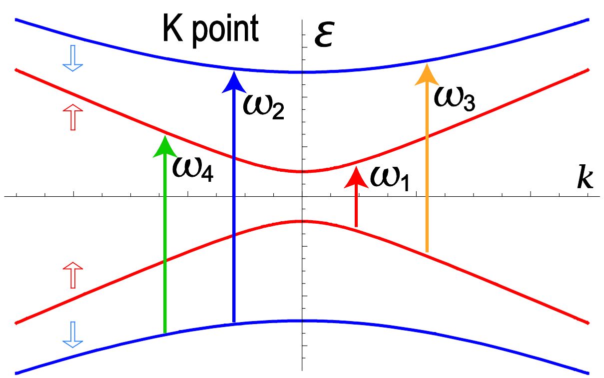

photo-induced transition from the valence band to the conduction band at the K point

M.Ezawa, Phys. Rev. B 86, 161407(R) (2012)

Electromagnetic potential

$$\boldsymbol{A}(t) = (A\sin\omega t, A\cos\omega t)$$

Covariant momentum $P_i \equiv \hbar k_i + eA_i$

$$H_\xi(A) = H_\xi + \mathcal{P}_x^\xi A_x + \mathcal{P}_y^\xi A_y$$

Circular polarization

$$\mathcal{P}_x^\xi = \frac{1}{\hbar}\frac{\partial H_\xi}{\partial k_x} = v_F \xi \tau_x - \frac{a\lambda_{R2}}{\hbar}\xi\tau_z\sigma_y,$$

$$\mathcal{P}_y^\xi = \frac{1}{\hbar}\frac{\partial H_\xi}{\partial k_y} = v_F \tau_y + \frac{a\lambda_{R2}}{\hbar}\xi\tau_z\sigma_x,$$

Silicene (monolayer honeycomb-silicon)

- Experimentally manufactured in 2012 (last year)
- Striking properties similar to graphene

  but more ramakable than graphene
- The low energy structure is described by Dirac fermions
- Buckled structure owing to a large ionic radius of silicon
- Relatively large spin-orbit gap of 3.9meV
- The band gap is controllable by applying the electric field
- The gap closes at a certain critical electric field
- Almost all topological phases can be materialized
- QHE, QSHE, QAHE, P-QHE(no LL), …..

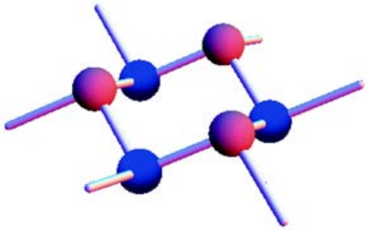

Skymions

- Skyrme introduced to explain how baryons could topologically emerge from a continuous meson field
- Skyrmions are solitons in a nonlinear field theory characterized by the topological quantum number
- Skyrmion is a nontrivial spin texture in 2D
- Homotopy class

$$S^2 \to S^2$$

$$\pi_2\left(S^2\right) = \mathbb{Z}$$

- Non zero Pontryagin number

$$Q_{\text{sky}} = -\frac{1}{8\pi}\sum_{ij}\int d^2x\varepsilon_{ij}\boldsymbol{n}(\boldsymbol{x})\cdot\left(\partial_i\boldsymbol{n}(\boldsymbol{x})\times\partial_j\boldsymbol{n}(\boldsymbol{x})\right)$$

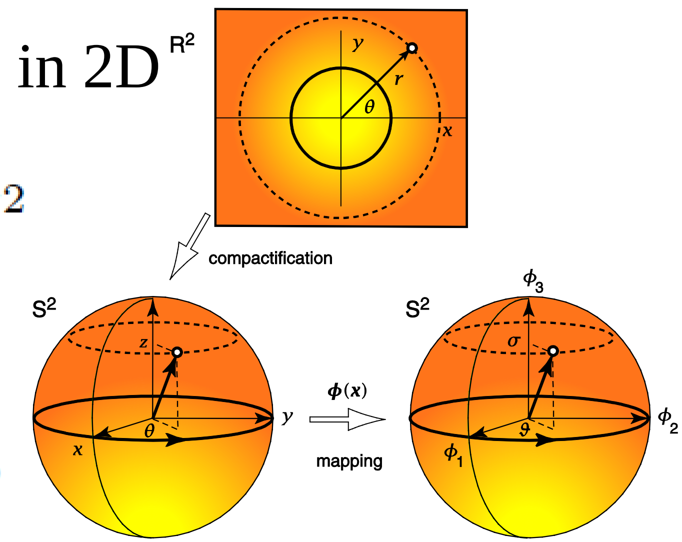

3x3 Si-Superstructure

K and K’ points become identical

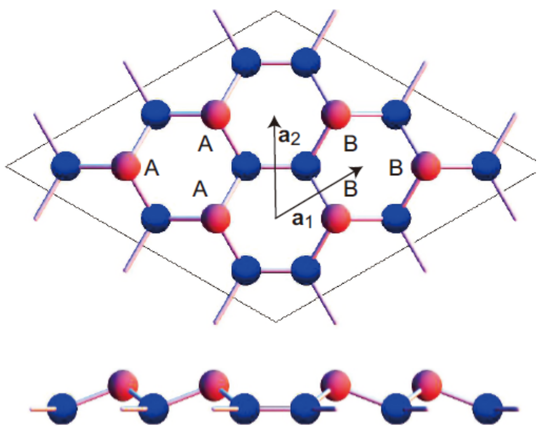

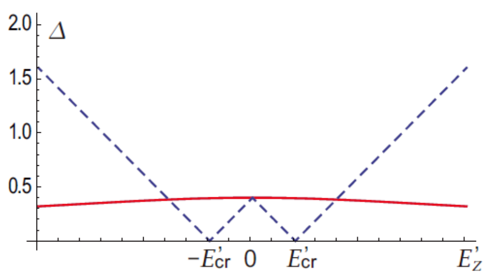

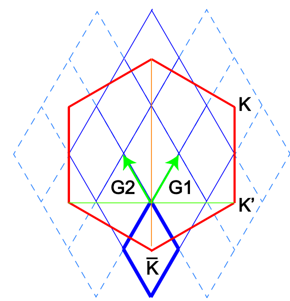

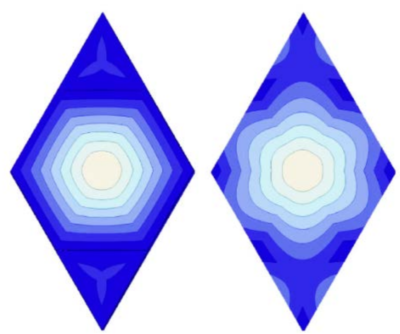

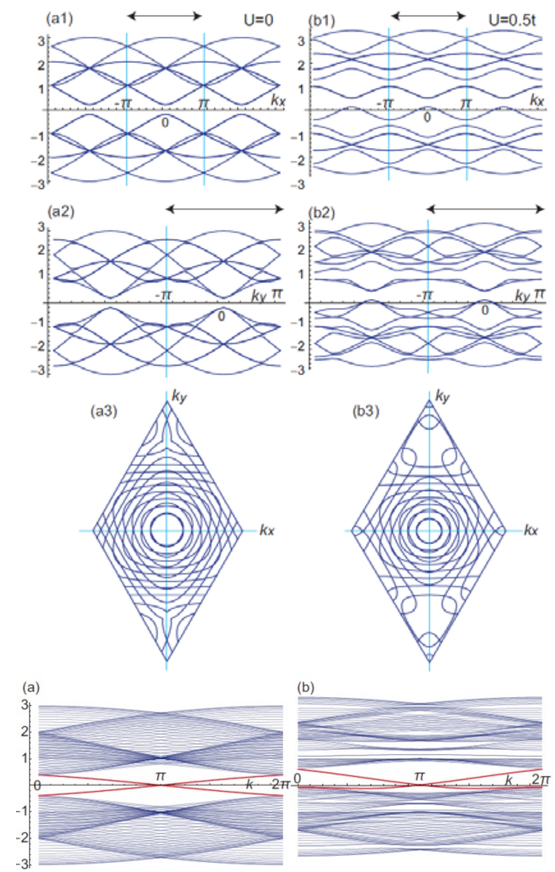

M.Ezawa, cond-mat/arXiv:1209.2580

Silicon Nanotube & Carbon Nanotube

Silicon nanotube is constructed by rolling up a silicene

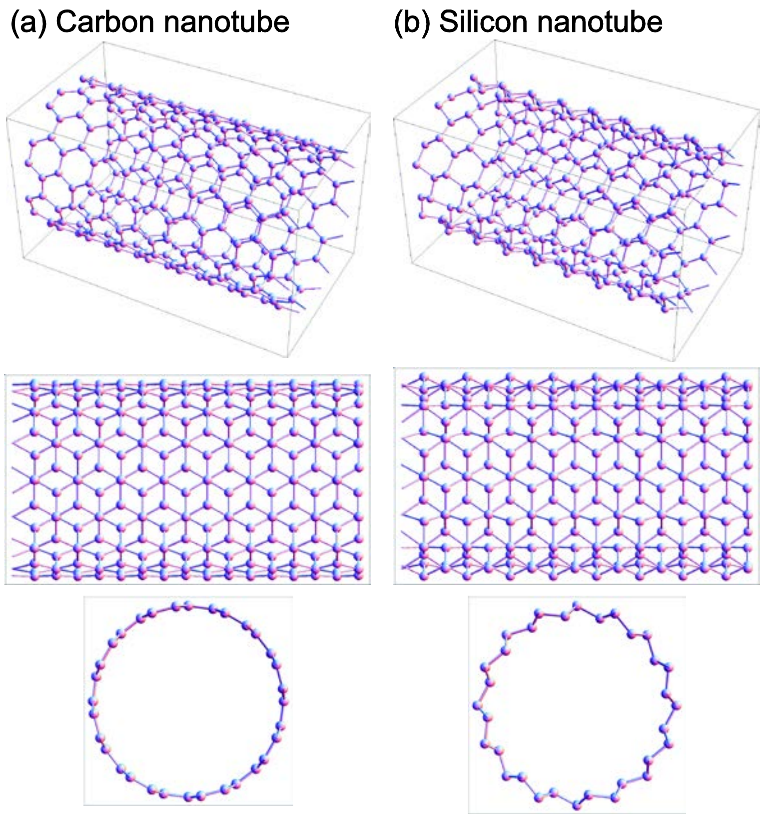

J. Sha, et.al., *Advanced Materials*, **14** 1219 (2002)

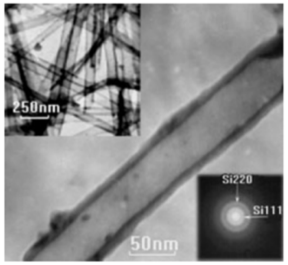

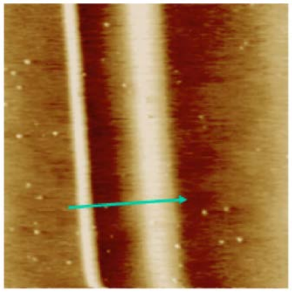

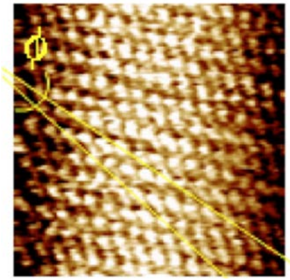

De Crescenzi et al. Appl. Phys. Lett. **86**, 231901 (2005)

M.Ezawa, Europhysics Letters 98, 67001 (2012)

Coupling the valley degree of freedom to antiferromagnetic order

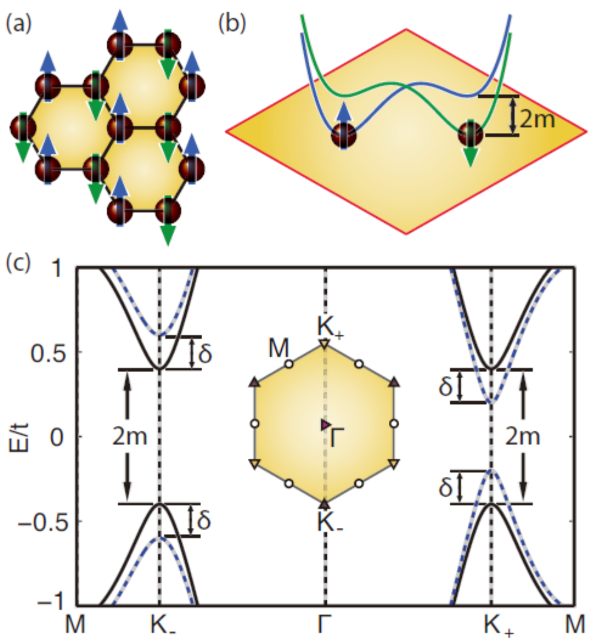

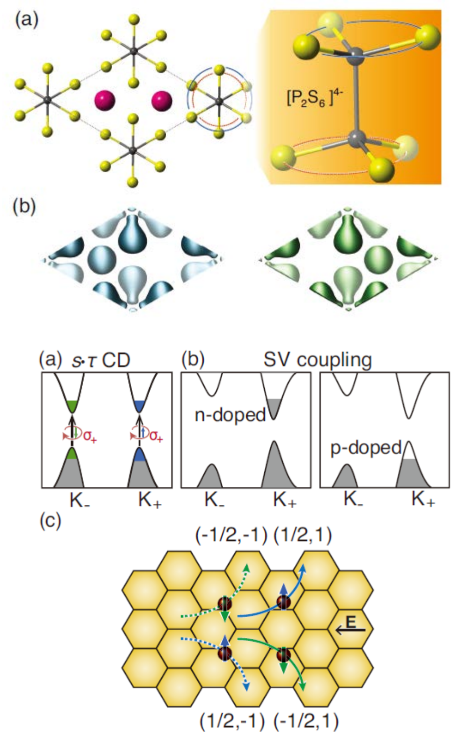

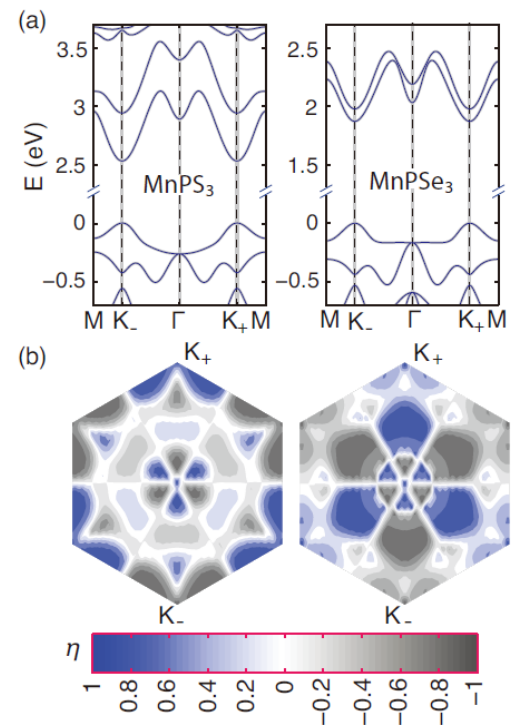

X. Li, T. Cao, Q. Niu, J. Shi, and J. Feng, cond-mat/arXiv:1210.4623

Inhomogeneous Electric Field

We apply the electric field $E_z(x)$ perpendicularly to a silicene sheet homogeneously in the y-direction and inhomogeneously in the x-direction.

- Helical Jackiw–Rebbi mode

$$\Psi(x,y) = e^{ik_y y}\Phi(x) \quad \phi_B(x) = i\xi\phi_A(x)$$

$$H_\eta\phi_A(x) = E_{\eta\xi}\phi_A(x) \quad E_{\eta\xi} = \eta\xi\hbar v_F k_y$$

Equation of motion

$$(\xi\hbar v_F\partial_x + \eta\lambda_{SO}\sigma_z - \ell E_z(x))\phi_A(x) = 0.$$

- Localized state

$$f(x) = C\exp\left[\frac{\xi}{\hbar v_F}\int^x (-\eta s_z\lambda_{SO} + \ell E_z(x'))\,dx'\right]$$

$$J_{s_z}(x) = \mathrm{Re}\left[\frac{\hbar}{2mi}\Psi^\dagger_{s_z}\partial_y\Psi_{s_z}\right] = \frac{\hbar k_y}{m}|\phi_{As_z}(x)|^2$$

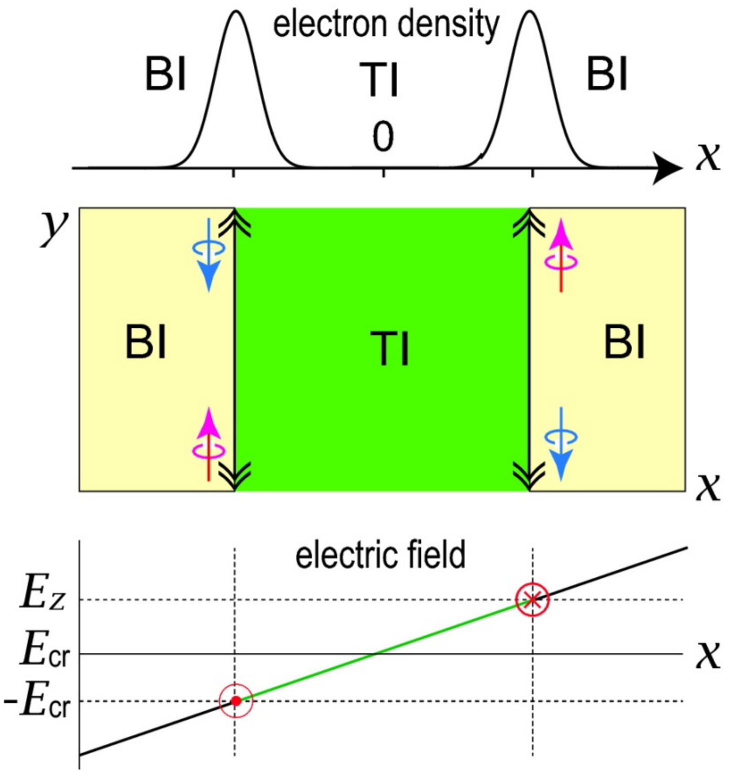

M.Ezawa, NJP 14 033003 (2012)

Perpendicular Electric Field

- Effective electric field is given by $E_z(x) = E\sin\theta$

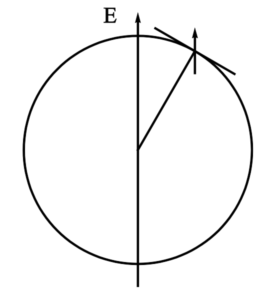

$$\left(\frac{2\pi}{L}\xi\hbar v_{\mathrm{F}}\partial_\theta - 2\ell E\cos\frac{\theta+\theta_j}{2}\sin\frac{\theta-\theta_j}{2}\right)\phi_A^{s_z}(\theta) = 0.$$

$$\phi_A^{s_z}(\theta) = C\exp\left[\frac{2L\ell E}{\pi\hbar v_{\mathrm{F}}}|\cos\theta_j|\cos\frac{\theta-\theta_j}{2}\right]$$

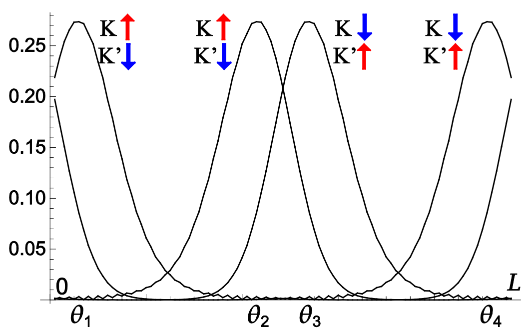

The wave function of each zero mode is localized within the metallic region

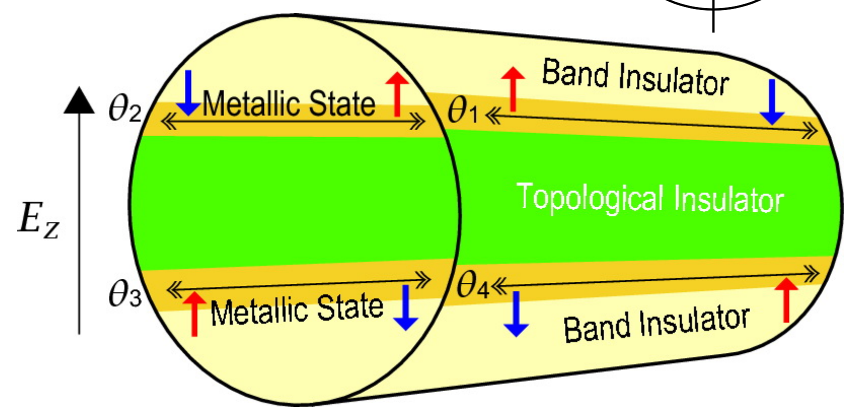

There emerge four helical zero modes propagating along the nanotube

M.Ezawa, Europhysics Letters 98, 67001 (2012)

Various Superstructures

$$\boldsymbol{g}_1 = p\boldsymbol{a}_1 + q\boldsymbol{a}_2, \qquad \boldsymbol{g}_2 = e^{\pm\pi/3}\boldsymbol{g}_1$$

$$|\boldsymbol{g}_1| = \sqrt{p^2 + q^2 + pq}$$

$$N = 2\,|\boldsymbol{g}_1|^2 = 2\left(p^2 + q^2 + pq\right)$$

$$\tan\phi = \sqrt{3}q/(2p+q)$$

Ag 145 pm
Si 111 pm
145/111=1.31

Ag-superstructure	Si-superstructure	p	q	ratio
$4 \times 4[1,2]$	3×3	3	0	1.33
$\sqrt{7} \times \sqrt{7}$	2×2	2	0	1.32
$\sqrt{13} \times \sqrt{13}[2]$	$\sqrt{7} \times \sqrt{7}$	2	1	1.36
$\sqrt{21} \times \sqrt{21}$	$2\sqrt{3} \times 2\sqrt{3}$	2	2	1.32
$2\sqrt{3} \times 2\sqrt{3}[17]$	$\sqrt{7} \times \sqrt{7}$	2	1	1.31
(free-standing)	1×1	1	0	
nothing	$\sqrt{3} \times \sqrt{3}$	1	1	

$$\boldsymbol{K} - \boldsymbol{K}' = n_1\boldsymbol{G}_1 + n_2\boldsymbol{G}_2$$

$$\boldsymbol{G}_1 = (\boldsymbol{g}_2 \times \boldsymbol{n})/\left|\boldsymbol{g}_1 \times \boldsymbol{g}_2\right|, \quad \boldsymbol{G}_2 = (\boldsymbol{g}_1 \times \boldsymbol{n})/\left|\boldsymbol{g}_1 \times \boldsymbol{g}_2\right|,$$

M.Ezawa, cond-mat/arXiv:1209.2580

Spin-Valley Polarized Metal

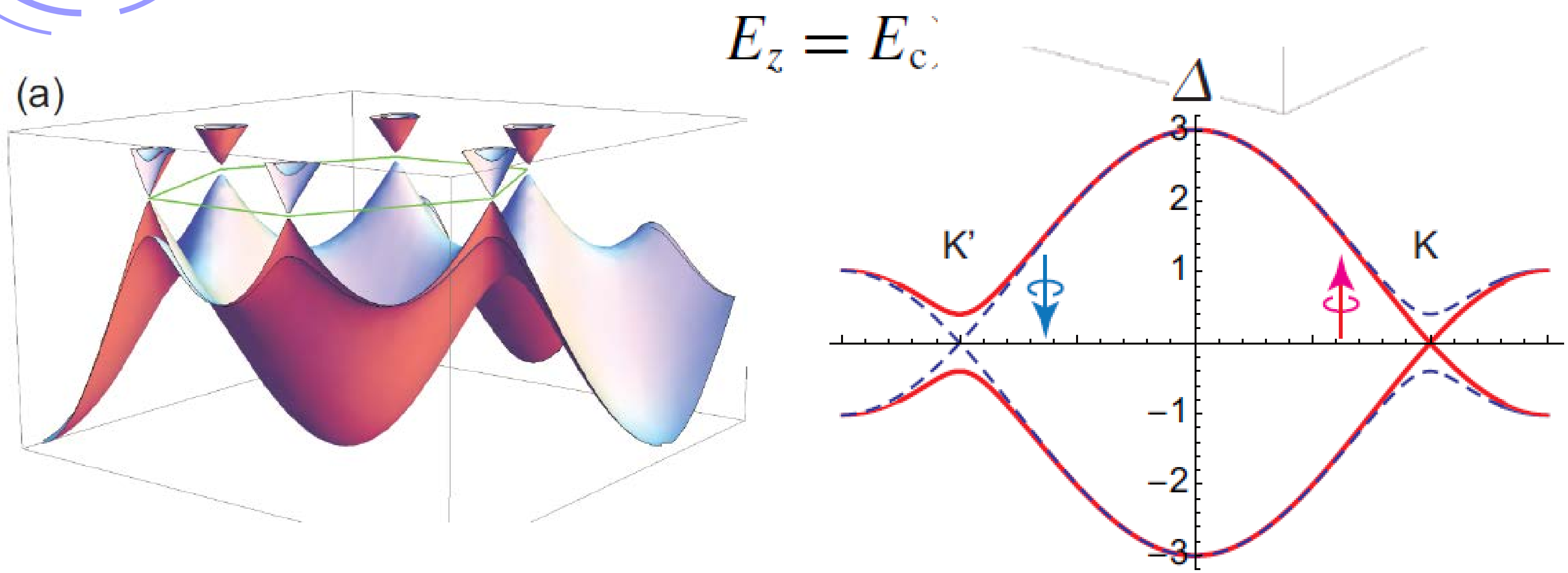

FIG. 3: (Color online) Band structure of silicene at the critical electric field E_c. (a) A bird's-eye view. Dirac cones are found at 6 corners of the hexagonal Brillouin zone. (b) The cross section containing a pair of K and K' points. The solid red (dashed blue) band is for up-spin (down-spin) electrons, which are gapless (gapped) at the K point but gapped (gapless) at the K' point.

M.Ezawa, NJP 14 033003 (2012)

Band Structure of Silicene Nanoribbon

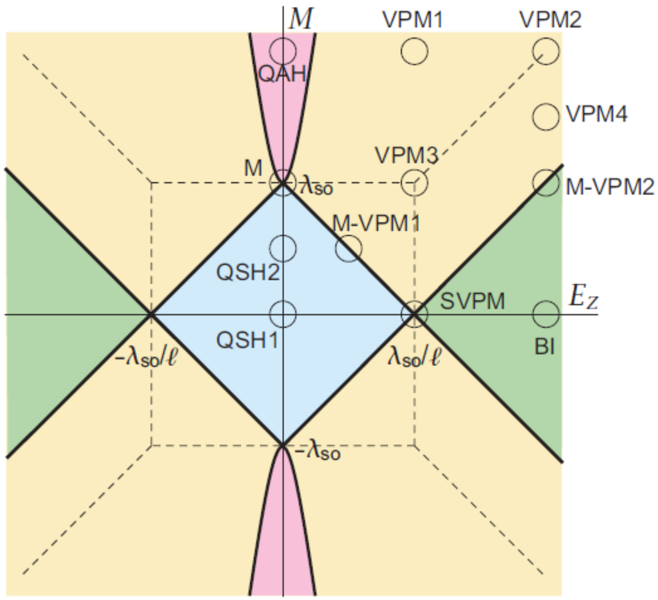

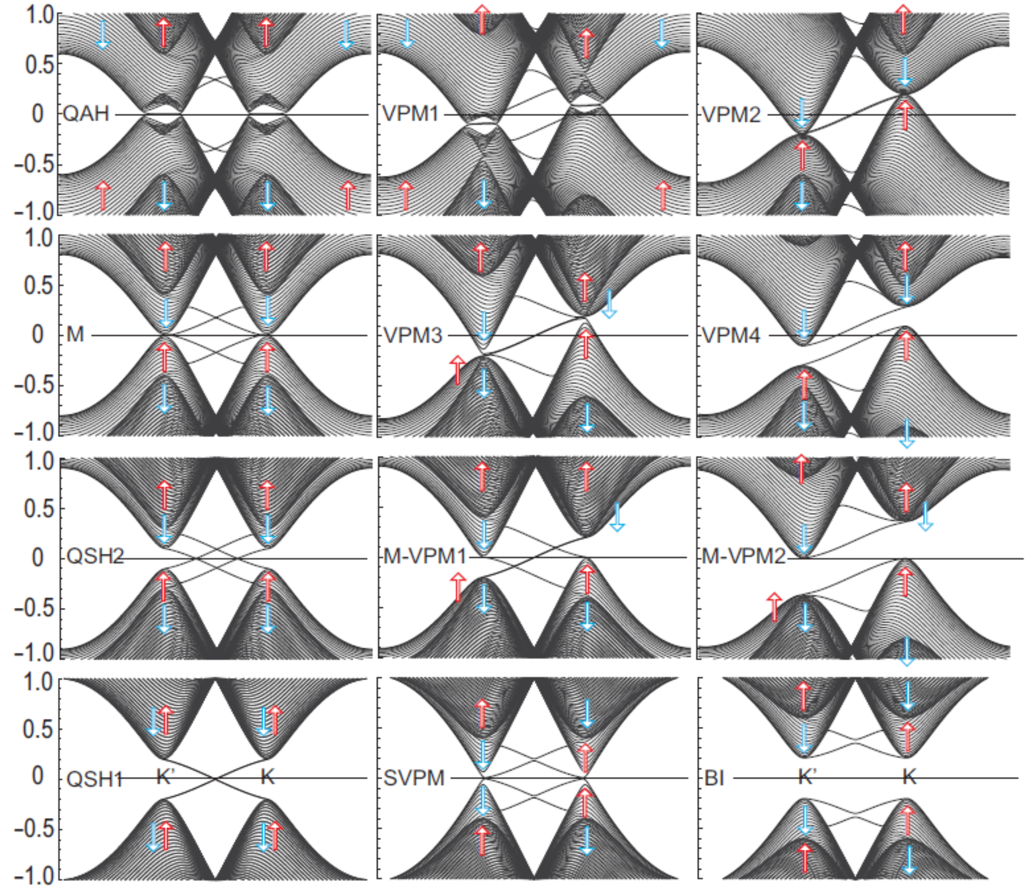

M.Ezawa, cond-mat/arXiv:1203.0705

Topological Insulator

- Topology charge is defined for an insulator
- Topological insulator has a nontrivial topological charge
- Surface has a gapless modes
- *Chiral* or *Helical* edge modes
- Quantum Hall effects $\longrightarrow$ chiral edge
- Quantum Spin Hall effects $\longrightarrow$ helical edge
- QAH effects

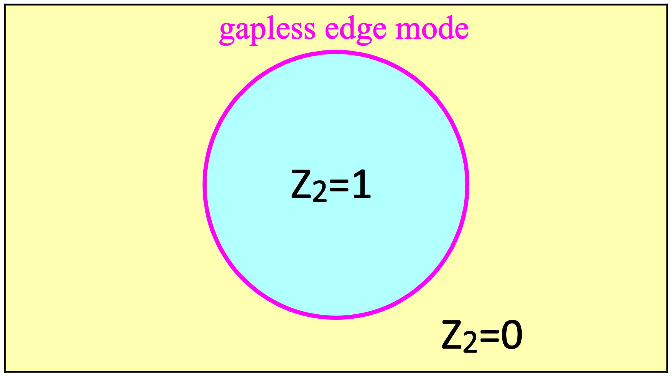

Bulk-Edge Correspondence

- If a bulk has a non-trivial topological number, the edge has gapless edge modes due to the discontinuity of the topological number.
- Quantum spin Hall effect ⇨ Helical zero modes

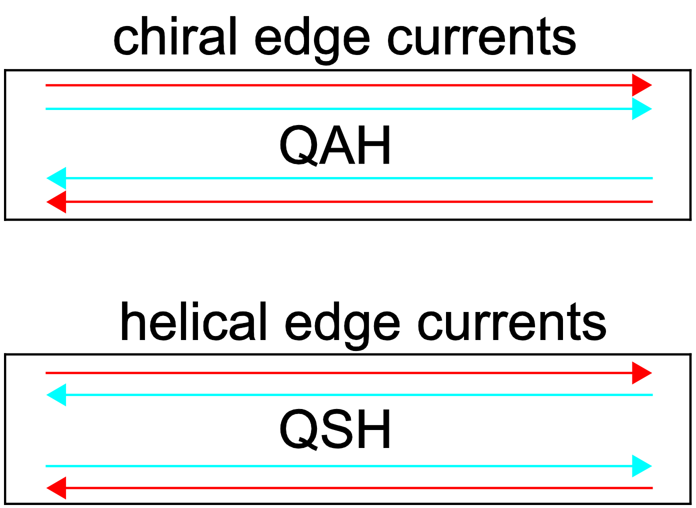

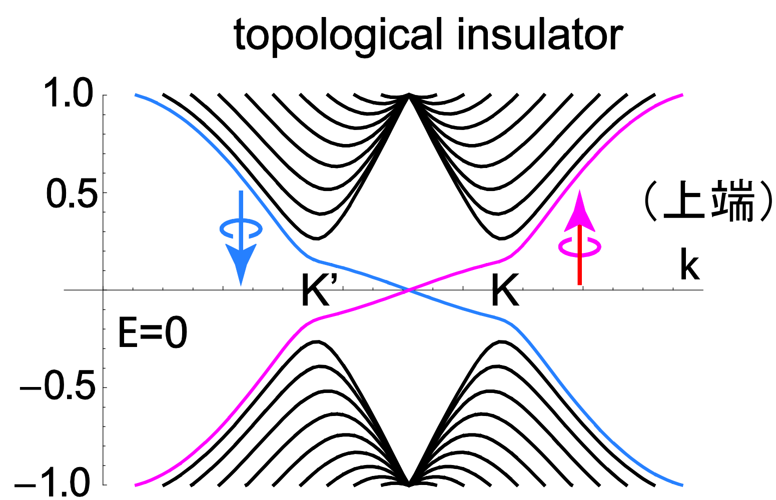

Chern Number and Meron

- SU(2) Hamiltonian $H = \boldsymbol{\tau} \cdot \boldsymbol{d}$
- Chern number
- Pontryagin number

$$\boxed{\mathcal{C} = \frac{1}{4\pi} \int d^2k \left(\frac{\partial \hat{\boldsymbol{d}}}{\partial k_x} \times \frac{\partial \hat{\boldsymbol{d}}}{\partial k_y} \right) \cdot \hat{\boldsymbol{d}}}$$

- Chern number is determined by the sign of Dirac mass

$$H = \begin{pmatrix} m_{\mathrm{D}} & \hbar v_{\mathrm{F}} \left(k_x + i k_y \right) \\ \hbar v_{\mathrm{F}} \left(k_x - i k_y \right) & -m_{\mathrm{D}} \end{pmatrix}$$

$$\mathcal{C}_{s_z}^{\eta} = \frac{\eta}{2} \mathrm{sgn} \left(m_{\mathrm{D}} \right)$$

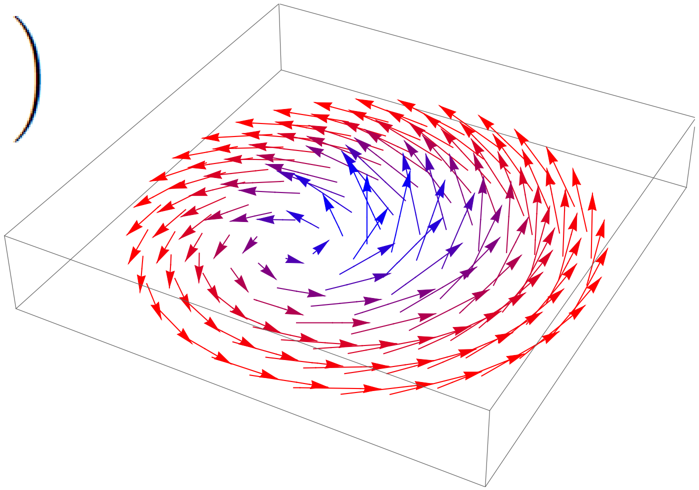

- Meron in momentum space
- Meron is a topological object with
  a half Pontyragin number

Phase Diagram in E-M plane

- Quantum spin Hall (QSH)
- Quantum anomalous Hall
- Valley polarized metal (VPM)
- Marginal-VPM
- Spin-Valley polarized metal
- Band insulator (BI)

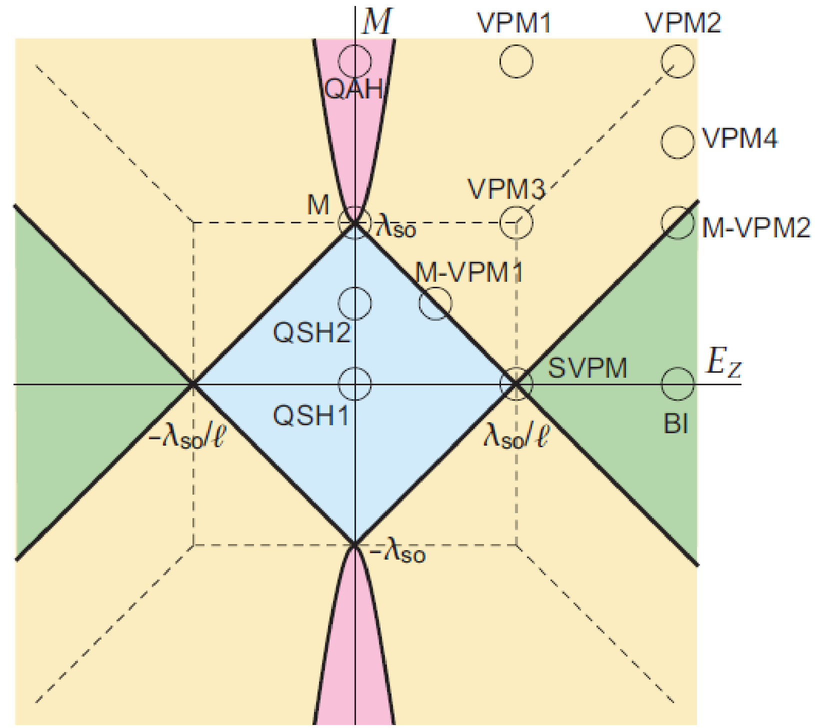

FIG. 1: (Color online) Phase diagram in the E_z-M plane. Dotted lines represent the points where the band gap closes. Heavy lines represent phase boundaries. A circle shows a point where the energy spectrum is calculated and shown in Fig.2.

M.Ezawa, cond-mat/arXiv:1203.0705 (to be publisehd in PRL)

Silicon Nanotube from Silicene

- Chiral vector $\mathbf{L} = n_1\mathbf{a}_1 + n_2\mathbf{a}_2$
- Nanotube circumference

$$L = |\mathbf{L}| = a\sqrt{n_1^2 + n_2^2 - n_1 n_2}$$

- Periodic boundary condition

$$\psi(x+L, y) = \psi(x, y)$$

- Descretization of k_x

$$k_x = 2\pi j/L \quad j = 0, 1, \cdots, 2n-1$$

- Brilloin zone $\quad -\pi/T \leq k_y \leq \pi/T$
- Energy spectrum of silicon nanotube

$$E_j(k_y) = \mathcal{E}(k_x, k_y)$$

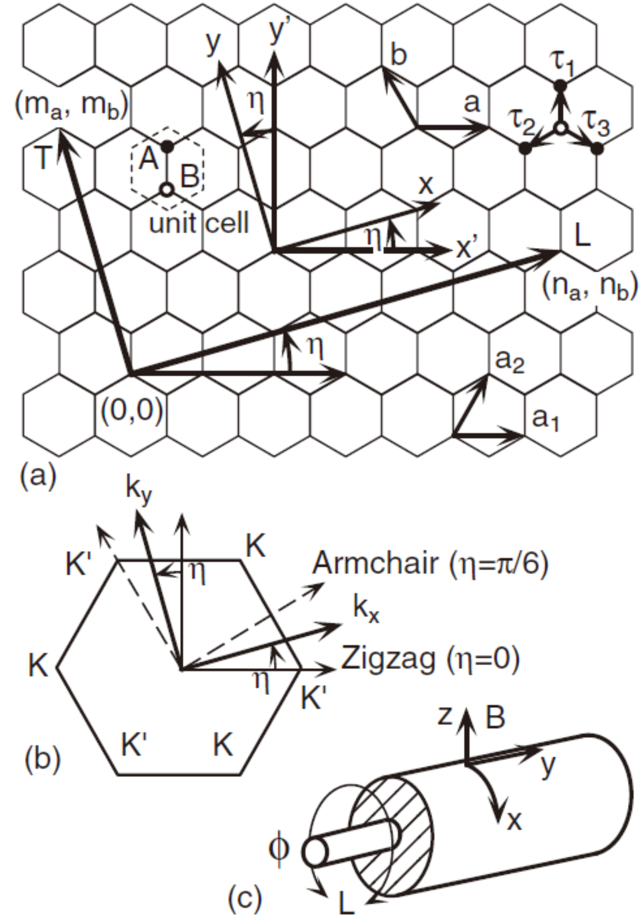

Zero-Energy Helical Modes

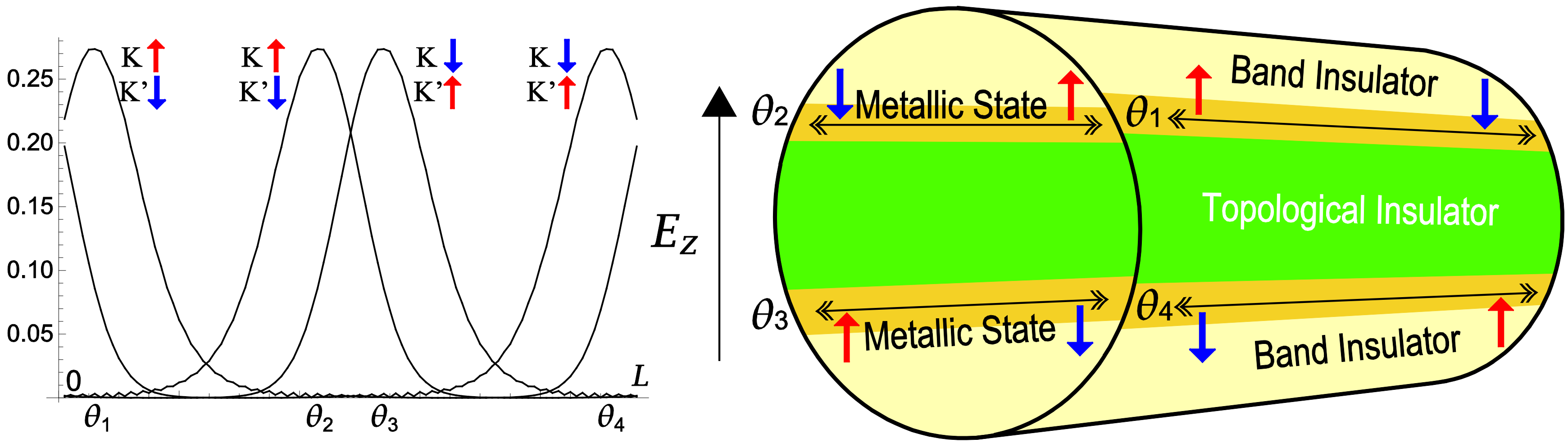

Fig. 5: (Color online) An illustration of silicon nanotube under electric field $E > E_{cr}$. There appear two topological insulator regions and two band insulator regions. They are separated by metallic states made of helical zero modes. A spin current flows in each metallic region as indicated. For instance, up-spin (down-spin) electrons propagate into the left (right) direction at $\theta = \theta_1$.

M.Ezawa, Europhysics Letters 98, 67001 (2012)

Silicon Nanotube vs Silicene Nanoribbon

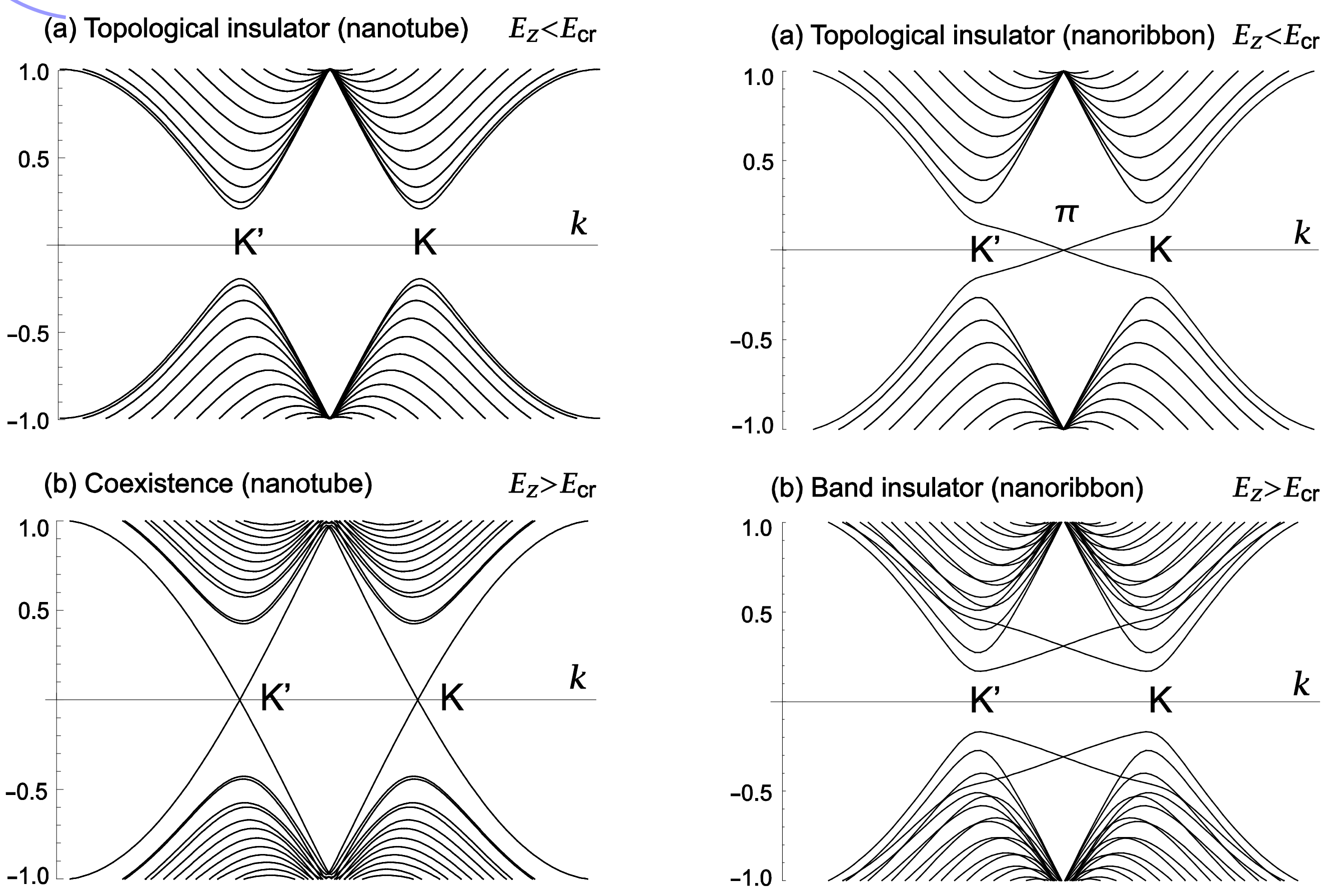

M.Ezawa, Europhysics Letters 98, 67001 (2012)

Quantum Hall Effects in Silicene

$$\hat{a} = \frac{\ell_B (P_x + i P_y)}{\sqrt{2}\hbar}, \quad \hat{a}^\dagger = \frac{\ell_B (P_x - i P_y)}{\sqrt{2}\hbar}$$

$$\begin{pmatrix} \Delta_+ (E_z) & \hbar\omega_c \hat{a} & i \frac{\sqrt{2}\hbar a \lambda_R}{\ell_B} \hat{a}^\dagger & 0 \\ \hbar\omega_c \hat{a}^\dagger & -\Delta_+ (E_z) & 0 & -i \frac{\sqrt{2}\hbar a \lambda_R}{\ell_B} \hat{a}^\dagger \\ -i \frac{\sqrt{2}\hbar a \lambda_R}{\ell_B} \hat{a} & 0 & \Delta_- (E_z) & \hbar\omega_c \hat{a} \\ 0 & i \frac{\sqrt{2}\hbar a \lambda_R}{\ell_B} \hat{a} & \hbar\omega_c \hat{a}^\dagger & -\Delta_- (E_z) \end{pmatrix}$$

$$\Psi_+^N = \left(u_{A\uparrow}^N \left| N \right\rangle, u_{B\uparrow}^{N+1} \left| N+1 \right\rangle, u_{A\downarrow}^{N-1} \left| N-1 \right\rangle, u_{B\downarrow}^N \left| N \right\rangle \right)^t$$

M.Ezawa, J. Phys. Soc. Jpn. 81, 064705 (2012)

Quantum Hall effects in Silicene

- 4-fold degenerate zero-energy states are completely resolved even without considering Coulomb interactions.

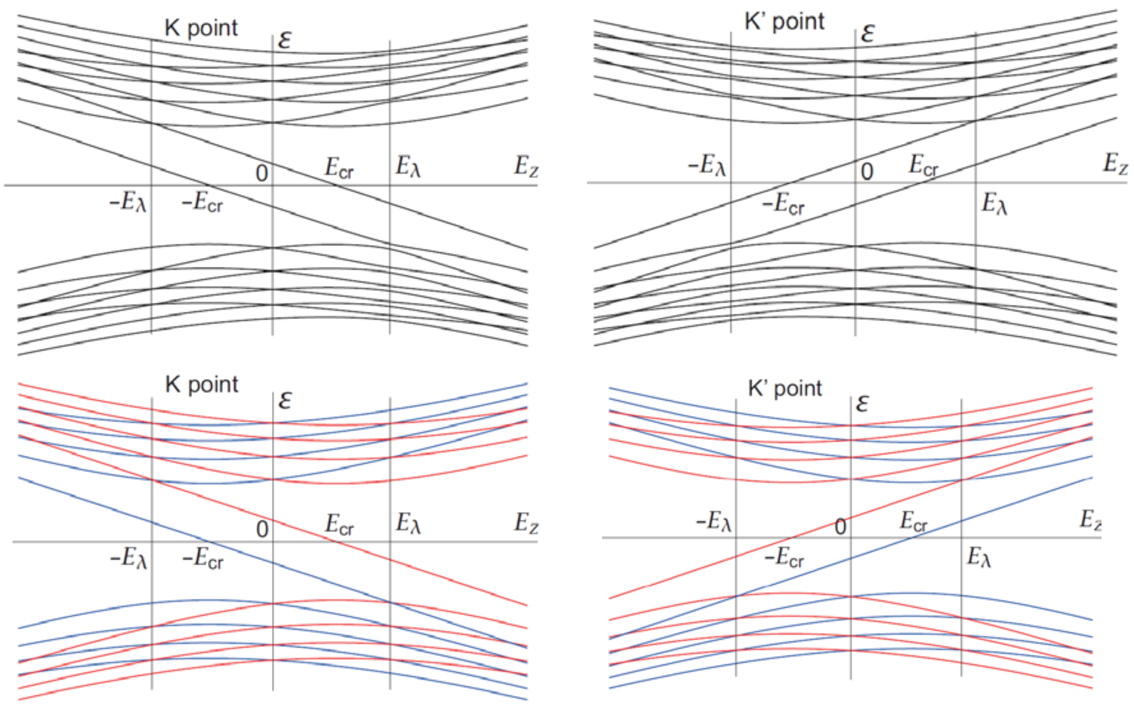

Without Rashba term

M.Ezawa, J. Phys. Soc. Jpn. 81, 064705 (2012)

Supersymmetric structure

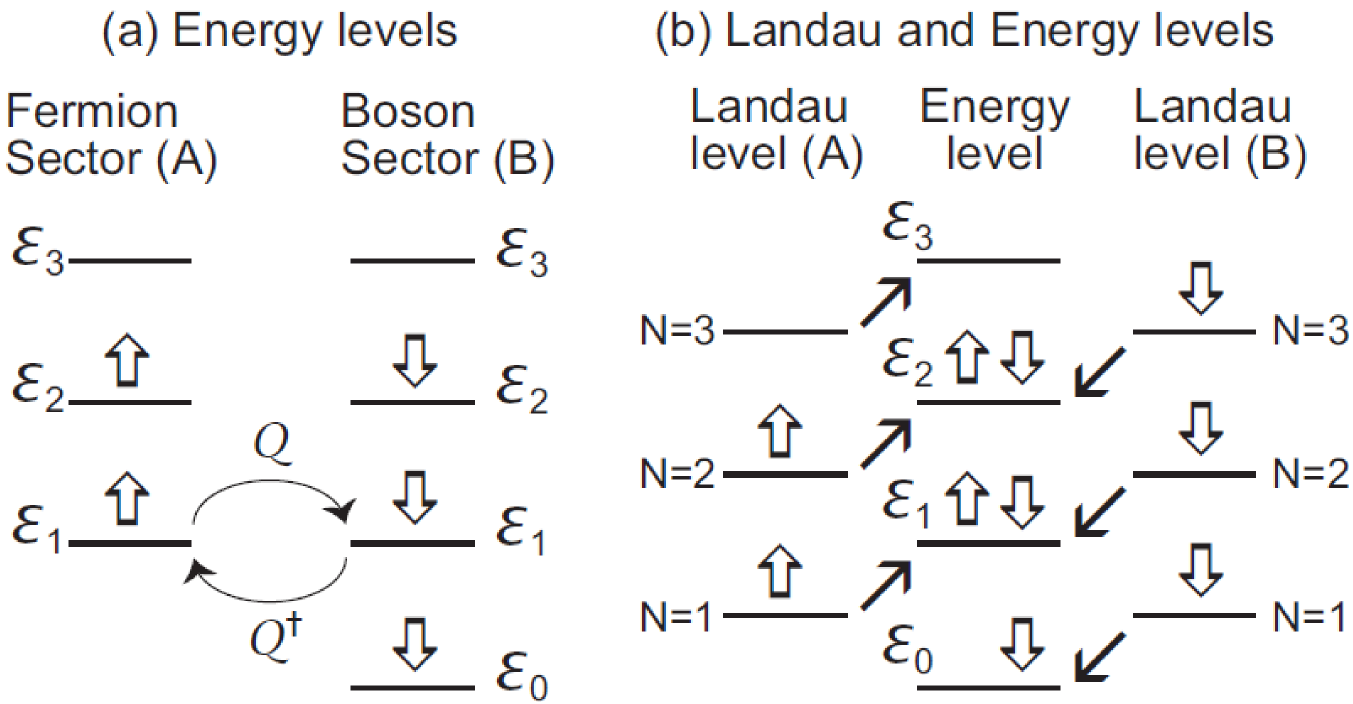

M.Ezawa, cond-mat/arXiv:1202.1357

Supersymmetric structure

$$H_\eta^{s_z} = \hbar\omega_c Q_{\eta s_z} + \tau_3 \Delta_{\eta s_z}$$

$$Q_+ = \begin{pmatrix} 0 & \hat{a} \\ \hat{a}^\dagger & 0 \end{pmatrix}, \quad Q_- = \begin{pmatrix} 0 & \hat{a}^\dagger \\ \hat{a} & 0 \end{pmatrix}$$

$$(H_\eta^{s_z})^2 = (\hbar\omega_c)^2 Q_{\eta s_z} Q_{\eta s_z} + \Delta_{\eta s_z}^2 (E_z)$$

$$H_P^+ = \begin{pmatrix} \hat{a}\hat{a}^\dagger & 0 \\ 0 & \hat{a}^\dagger\hat{a} \end{pmatrix}$$

M.Ezawa, cond-mat/arXiv:1202.1357

$$Q = \begin{pmatrix} 0 & 0 \\ \hat{a}^\dagger & 0 \end{pmatrix}, \qquad Q^\dagger = \begin{pmatrix} 0 & \hat{a} \\ 0 & 0 \end{pmatrix}$$

$$H_{\mathrm{P}}^{+} = \{Q, Q^\dagger\}, \qquad \left[H_\eta^{+}, Q\right] = 0$$

$$H_{\mathrm{P}}^{+} = \hat{a}^\dagger \hat{a} + \hat{c}^\dagger \hat{c} \qquad \hat{c} = \begin{pmatrix} 0 & 0 \\ 1 & 0 \end{pmatrix}, \qquad \hat{c}^\dagger = \begin{pmatrix} 0 & 1 \\ 0 & 0 \end{pmatrix}$$

$$\hat{c}|0\}_B = 0, \quad \hat{c}^\dagger|0\}_B = |0\}_A, \quad \hat{c}|0\}_A = |0\}_B$$

$$|N\}_A = \frac{1}{\sqrt{N!}} \hat{a}^{\dagger N}|0\}_A = \begin{pmatrix} |N\rangle \\ 0 \end{pmatrix} \qquad |N\}_B = \frac{1}{\sqrt{N!}} \hat{a}^{\dagger N}|0\}_B = \begin{pmatrix} 0 \\ |N\rangle \end{pmatrix}$$

M.Ezawa, cond-mat/arXiv:1202.1357

Energy level

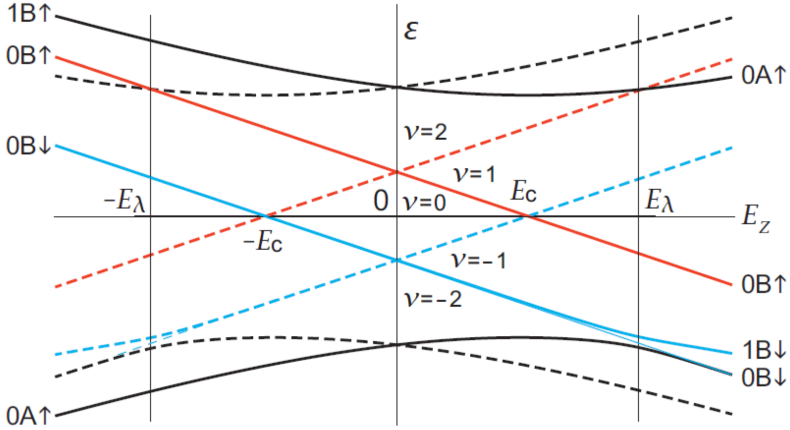

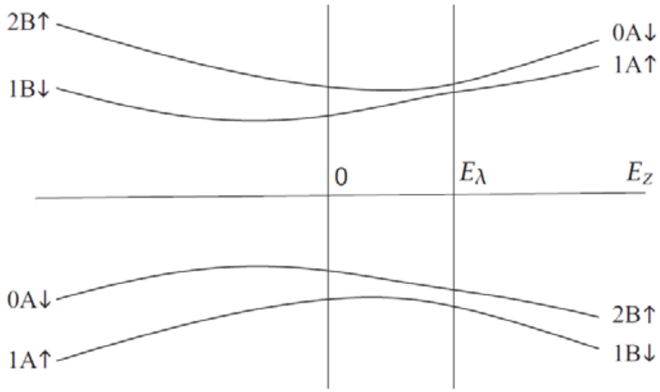

M.Ezawa, cond-mat/arXiv:1202.1357

Dirac Fermions on Zigzag Edge

$$v_F \begin{pmatrix} 0 & p_x - ip_y \\ p_x + ip_y & 0 \end{pmatrix} \begin{pmatrix} \phi_A^K(\boldsymbol{x}) \\ \phi_B^K(\boldsymbol{x}) \end{pmatrix} = E \begin{pmatrix} \phi_A^K(\boldsymbol{x}) \\ \phi_B^K(\boldsymbol{x}) \end{pmatrix}$$

$$v_F \begin{pmatrix} 0 & -p_x - ip_y \\ -p_x + ip_y & 0 \end{pmatrix} \begin{pmatrix} \phi_A^{K'}(\boldsymbol{x}) \\ \phi_B^{K'}(\boldsymbol{x}) \end{pmatrix} = E \begin{pmatrix} \phi_A^{K'}(\boldsymbol{x}) \\ \phi_B^{K'}(\boldsymbol{x}) \end{pmatrix}$$

$$p_x - ip_y = -2i\hbar\partial_z, \qquad p_x + ip_y = -2i\hbar\partial_{z^*}$$

$$\partial_{z^*}\phi_A^K(\boldsymbol{x}) = i\frac{E}{2\hbar}\phi_B^K(\boldsymbol{x}), \qquad \partial_z\phi_B^K(\boldsymbol{x}) = i\frac{E}{2\hbar}\phi_A^K(\boldsymbol{x}),$$

$$\partial_z\phi_A^{K'}(\boldsymbol{x}) = -i\frac{E}{2\hbar}\phi_B^{K'}(\boldsymbol{x}), \quad \partial_{z^*}\phi_B^{K'}(\boldsymbol{x}) = -i\frac{E}{2\hbar}\phi_A^{K'}(\boldsymbol{x}).$$

Cauchy-Riemann eq

Wave functions are holomorphic or antiholomorphic for E=0